Pediatric Radiology
https://doi.org/10.1007/s00247-020-04721-1

PICTORIAL ESSAY

Intracranial calcifications in childhood: Part 1

Fabrício Guimarães Gonçalves[1] · Luca Caschera[2] · Sara Reis Teixeira[1] · Angela Nicole Viaene[3] · Lorenzo Pinelli[4] · Kshitij Mankad[5] · César Augusto Pinheiro Ferreira Alves[1] · Xilma Rosa Ortiz-Gonzalez[6,7] · Savvas Andronikou[1,8] · Arastoo Vossough[1,8]

Received: 6 February 2020 / Revised: 3 April 2020 / Accepted: 12 May 2020

Abstract

This article is the first of a two-part series on intracranial calcification in childhood. Intracranial calcification can be either physiological or pathological. Physiological intracranial calcification is not an expected neuroimaging finding in the neonatal or infantile period but occurs, as children grow older, in the pineal gland, habenula, choroid plexus and occasionally the dura mater. Pathological intracranial calcification can be broadly divided into infectious, congenital, endocrine/metabolic, vascular and neoplastic. The main goals in Part 1 are to discuss the chief differences between physiological and pathological intracranial calcification, to discuss the histological characteristics of intracranial calcification and how intracranial calcification can be detected across neuroimaging modalities, to emphasize the importance of age at presentation and intracranial calcification location, and to propose a comprehensive neuroimaging approach toward the differential diagnosis of the causes of intracranial calcification. Finally, in Part 1 the authors discuss the most common causes of infectious intracranial calcification, especially in the neonatal period, and congenital causes of intracranial calcification. Various neuroimaging modalities have distinct utilities and sensitivities in the depiction of intracranial calcification. Age at presentation, intracranial calcification location, and associated neuroimaging findings are useful information to help narrow the differential diagnosis of intracranial calcification. Intracranial calcification can occur in isolation or in association with other neuroimaging features. Intracranial calcification in congenital infections has been associated with clastic changes, hydrocephalus, chorioretinitis, white matter abnormalities, skull changes and malformations of cortical development. Infections are common causes of intracranial calcification, especially neonatal TORCH (toxoplasmosis, other [syphilis, varicella-zoster, parvovirus B19], rubella, cytomegalovirus and herpes) infections.

Keywords Brain · Calcification · Children · Computed tomography · Infection · Intracranial · Magnetic resonance imaging · Neurocutaneous syndrome · Physiological · Ultrasound

CME activity This article has been selected as the CME activity for the current month. Please visit the SPR website at www.pedrad.org on the Education page and follow the instructions to complete this CME activity.

✉ Fabrício Guimarães Gonçalves
goncalves.neuroradio@gmail.com

[1] Department of Radiology, Division of Neuroradiology, Children's Hospital of Philadelphia, 3401 Civic Center Blvd., Philadelphia, PA 19104, USA

[2] Fondazione IRCCS Ca' Granda Ospedale Maggiore Policlinico, Neuroradiology Unit, Milan, Italy

[3] Department of Pathology and Laboratory Medicine, Children's Hospital of Philadelphia, University of Pennsylvania Perelman School of Medicine, Philadelphia, PA, USA

[4] Neuroradiology Unit, Pediatric Neuroradiology Section, ASST Spedali Civili, Brescia, Italy

[5] Department of Radiology, Great Ormond Street Hospital, London, UK

[6] Department of Pediatrics, Division of Neurology, Children's Hospital of Philadelphia, Philadelphia, PA, USA

[7] Department of Neurology, University of Pennsylvania Perelman School of Medicine, Philadelphia, PA, USA

[8] Department of Radiology, Perelman School of Medicine, University of Pennsylvania, Philadelphia, PA, USA

Published online: 30 July 2020

Introduction

Nonosseous calcium is vital in intra- and extracellular signaling, vascular constriction and vasodilation, hormone secretion, nerve impulse transmission, and muscle contraction [1]. Calcium homeostasis plays crucial roles in the homeostasis of other elements (e.g., phosphorus), in different pathways of neuroinflammation and neurodegeneration, and cell death regulation [2, 3]. Moreover, it is well known that cellular necrosis can be precipitated by intracellular calcium overload, leading to mitochondrial damage and cellular collapse [4, 5].

Recently, McCartney and Squier [6] performed a postmortem histopathological study in fetuses, infants and older children, examining intracranial calcium deposits across a range of conditions including hypoxic–ischemic encephalopathy, infections and genetic abnormalities. They reported that brain calcifications can be either dystrophic or vascular (Fig. 1) [6]. Dystrophic calcification is a result of uncontrolled calcium influx into necrotic cells, often following ischemia and infections. Vascular calcification, which might also be associated with ischemia, appears to begin in protein droplets adjacent to, or within, the walls of small blood vessels. Calcifications not associated with tissue necrosis would be initiated in intracellular protein globules, outside the endothelium of small vessels, possibly in pericytes, which might explain the association with atrophy, gliosis and cortical maldevelopment [6].

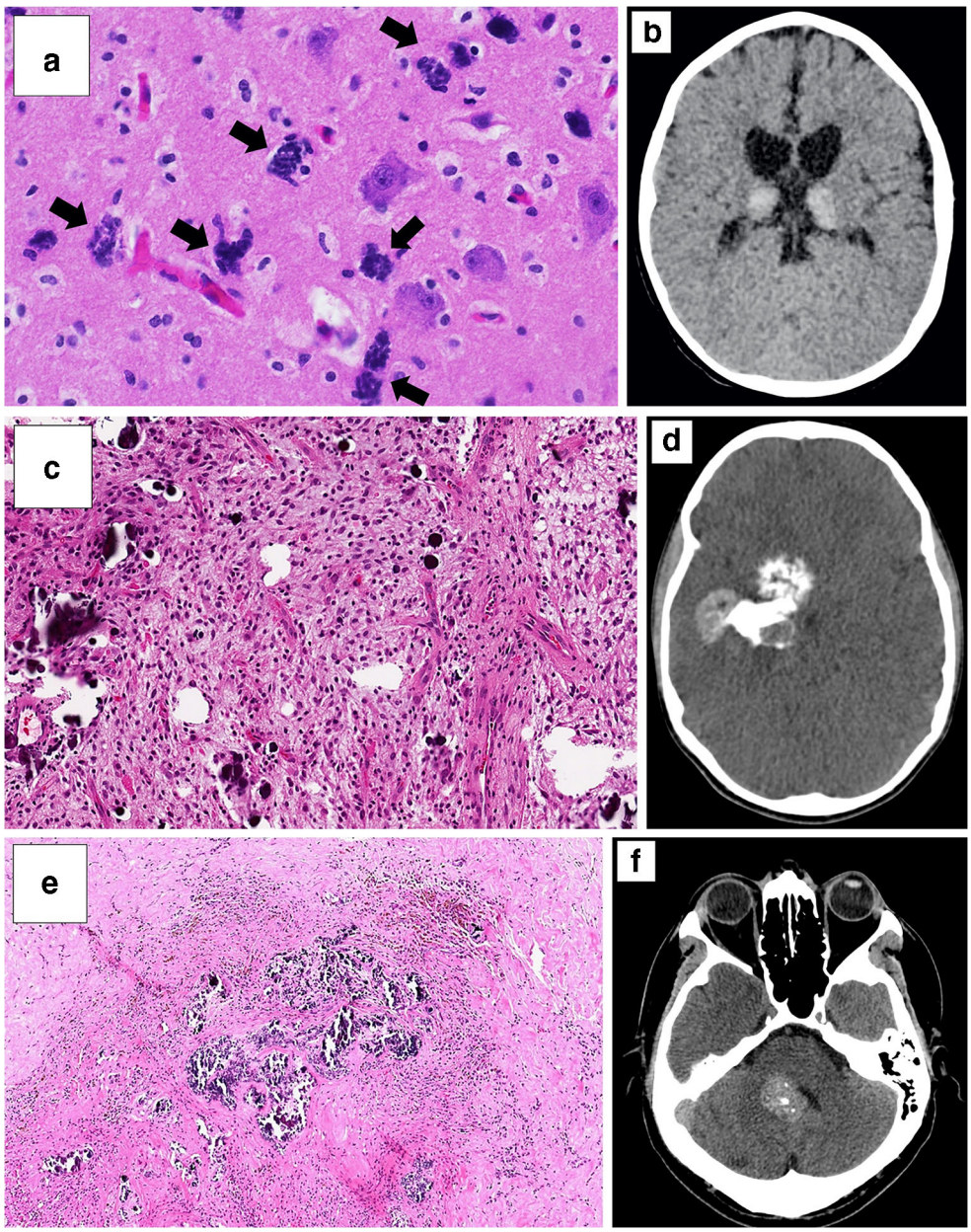

Fig. 1 Intracranial calcifications. **a** Histological example of intracranial calcifications shows mineralization of thalamic neurons (*arrows*) in an 11-month-old boy with global hypoxic–ischemic brain injury (hematoxylin and eosin [H&E] stain, 400x magnification). **b** Nonenhanced axial CT image shows bilateral thalamic increased density in the same patient at 12 months old, in keeping with calcification from hypoxic–ischemic brain injury. **c**, **d** Numerous calcifications within a ganglioglioma in a 6-year-old girl, World Health Organization (WHO) Grade 1 (H&E stain, 100x magnification; **c**), and corresponding nonenhanced axial CT (**d**), show a heavily calcified large lobulated heterogeneous mass in the right medial temporal lobe. **e**, **f** Parenchymal calcifications found along a cavernous malformation (H&E stain, 50x magnification; **e**) in a 12-year-old girl and corresponding nonenhanced axial CT image (**f**) show a large dense and partially calcified mass in the right medial cerebellar peduncle and cerebellar hemisphere, projecting into the 4th ventricle

Intracranial calcification occurs in the brain parenchyma, meninges and choroid plexus, and within vessel walls [7]. Intracranial calcification can be categorized into six groups: physiological, infectious, congenital, endocrine/metabolic, vascular and neoplastic [8]. Notwithstanding its cause, intracranial calcification is often a nonspecific neuroimaging feature that generally requires correlation with age at presentation, location and further neuroimaging findings, to narrow the differential diagnosis.

This review comprises two parts. Part 1 is a brief overview of the imaging diagnosis of intracranial calcification, describing the main differences between physiological and pathological intracranial calcification, depicting the relevance of age at presentation, emphasizing the importance of the location of intracranial calcification, and providing a comprehensive neuroimaging approach toward the differential diagnosis. This stepwise approach takes into consideration the presence of additional neuroimaging and clinical findings (e.g., cortical malformations, clastic changes, vascular malformations, overriding sutures, hydrocephalus, cortical changes, white matter changes, mass lesions and skin changes). Congenital and infectious causes of intracranial calcification are also discussed in Part 1. Part 2 focuses on endocrine/metabolic, vascular and neoplastic causes of intracranial calcification.

Brief overview on imaging diagnosis of intracranial calcifications

Various neuroimaging modalities have distinct utilities and sensitivities in depicting intracranial calcification. Plain radiographs might demonstrate denser intracranial calcium deposits, including both physiological and pathological, with limited sensitivity given the presence of the overlying skull. US imaging can provide real-time evaluation of intracranial calcification; US depiction often depends on the presence of a sonographic window through a patent fontanelle. As such, this might not be feasible in older children. Calcifications typically appear as hyperechoic foci in the brain, with or without posterior acoustic shadowing. Therefore, they might, at times, be confused with areas of hemorrhage or other hyperechoic pathologies. However, small and subtle forms of calcification can sometimes be well delineated by modern high-resolution US techniques [9, 10] (Fig. 2), and occasionally better than with CT.

Computed tomography is a very sensitive method for depicting intracranial calcification. Increased attenuation is the hallmark of intracranial calcification, but specific Hounsfield units depend on the extent and density of the calcified regions. Less dense areas of high attenuation might occasionally mimic acute/subacute hemorrhage. However, often other clues assist in differentiation, such as the nature of the lesion, attenuation of the surrounding areas, edema and mass effect. Small, very dense foci of hyperattenuation are almost always caused by calcifications rather than hemorrhage. Generally, in conventional nonenhanced CT, any lesion with a density larger than 100 Hounsfield units (HU) is classified as calcification. Nevertheless, in lesions with density smaller than 100 HU, there is an overlap in blood and calcification [11].

Dual-energy CT is a relatively recent imaging technique with several advantages over conventional single-energy CT. Dual-energy CT can potentially provide a considerable reduction of beam-hardening effects, reconstruction of accurate monochromatic images and material decomposition images, and detailed material composition assessment by using X-ray spectral information. Material decomposition images in dual-energy CT can be useful for differentiating among high-density materials such as contrast material, calcification and fresh hematoma [12]; distinguishing iodine enhancement from calcification; and characterizing renal calculi [13]. By collecting attenuation information at two distinct energies, assumptions can be made about the shape of the energy-dependent attenuation curve for a given tissue, and thus about its material characteristics. Dual-contrast energy can discriminate calcification and hemorrhage in an intracranial lesion with a density below 100 HU or in other complex cases, with relatively high sensitivity, specificity and accuracy [13, 14].

Intracranial calcifications demonstrate a variable appearance on MRI. Conventional T1-weighted and T2-weighted imaging have limited sensitivity for the delineation of subtle or smaller calcium deposits. On T1-weighted imaging, calcified lesions might appear hypo- or hyperintense, depending on the molecule in which calcium is bound, the surface area of the particles, and calcium concentration. On T2-weighted imaging, calcifications are often hypointense [13, 14]. Calcium is a mildly diamagnetic substance and hence has a negative susceptibility. On gradient echo sequences optimized for T2* contrast, calcification demonstrates susceptibility, and as such, might have similar features to other forms of mineralization and blood products, including iron-containing paramagnetic substances. As a general rule, calcifications show fewer susceptibility blooming artifacts compared to blood products, but again form and density are essential factors in the neuroimaging appearance.

Susceptibility-weighted imaging is a gradient echo technique with a specific post-processing technique to maximize the sensitivity to susceptibility effects utilizing both magnitude and phase information. This combination makes this sequence quite sensitive in demonstrating susceptibility. The most common use of susceptibility-weighted imaging is for the depiction of small amounts of hemorrhage/blood products or calcium deposits, neither of which might be evident on other MR sequences. Both calcium deposits and blood

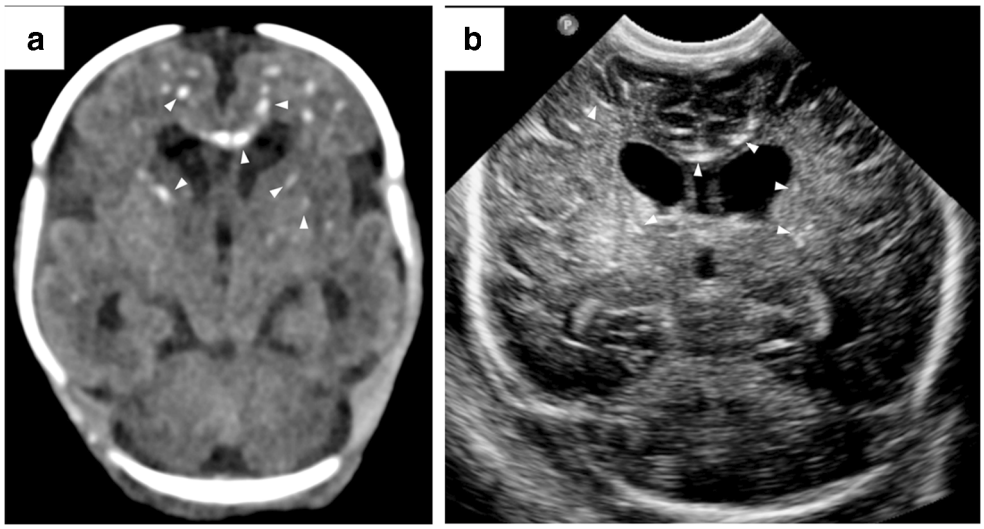

Fig. 2 US and CT imaging in a 3-day-old boy with a history of intrauterine growth restriction, hepatomegaly and thrombocytopenia from intrauterine cytomegalovirus (CMV) infection. **a** Nonenhanced axial CT image shows multiple small calcification foci in the subcortical white matter of the frontal lobes, corpus callosum and basal ganglia (*arrowheads*). **b** Coronal US image shows similar imaging findings (*arrowheads*)

products demonstrate low signal and often blooming artifacts on the magnitude images. The phase information, however, is, in most cases, able to distinguish between the two because diamagnetic and paramagnetic compounds alter phase information distinctively. In the phase image, vessels (veins and arteries) demonstrate similar signal intensity to blood products and the opposite signal intensity of calcium deposits. Susceptibility-weighted imaging typically involves a 3-D gradient echo sequence with a long echo time (TE), short repetition time (TR), small flip angle, high resolution, and full velocity compensation. Filtered phase images from susceptibility-weighted imaging have the potential to distinguish calcifications (diamagnetic) from blood products (paramagnetic). Depending on whether the imaging system is a left- or right-hand system, the low signal susceptibility on magnitude images shows high or low signal on the phase images, respectively (Fig. 3). The handedness of the MRI system determines whether calcification or blood is hyperintense or hypointense on the phase images, and the handedness is dependent on the MRI system vendor. Higher field strengths might increase sensitivity to detection of susceptibility, whereas the use of fast spin-echo sequences with multiple refocusing pulses, higher readout bandwidth, and lower echo time decreases the sensitivity.

According to the American College of Radiology appropriateness criteria, CT of the brain is superior to MRI for detecting calcification [15]. When MRI is performed, the inclusion of gradient echo or susceptibility-weighted imaging markedly improves the detection and assessment of not only calcifications but also microhemorrhages and intravascular thrombosis. There should be an effort to minimize unnecessary radiation exposure, particularly in children. An alternative modality should be considered when possible. CT should be minimized in cancer predisposition syndromes [16]. Other conditions that

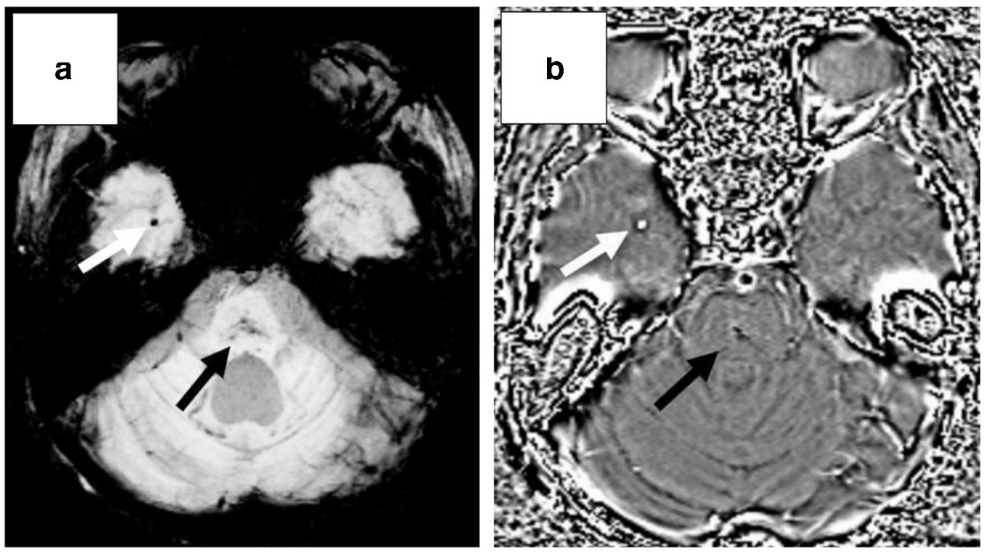

Fig. 3 Susceptibility-weighted imaging with magnitude and phase images in a 13-year-old boy previously treated for a brain tumor. **a** Magnitude image shows hypointense foci in the pons (*black arrow*) and the right temporal lobe (*white arrow*). **b** Phase image of this left-hand (Siemens) system distinguishes calcium, which remains hypointense in the pons (*black arrow*), and blood products, which are hyperintense in the temporal lobe (*white arrow*)

Table 1 Physiological and pathological categories of intracranial calcification in childhood

Six categories of intracranial calcification	
Physiological	• Physiological (habenula, pineal gland, choroid plexus, dura mater)
Pathological	• Infectious (pre- and postnatal infections)
	• Congenital (phakomatosis/chromosomal)
	• Endocrine/metabolic (parathyroid and thyroid hormone abnormalities/mitochondrial disorders/pseudo-TORCH syndromes/leukodystrophies/familial idiopathic basal ganglia calcification)
	• Vascular (vascular malformations/vasculopathies/vascular insults)
	• Neoplastic/radiation therapy

TORCH toxoplasmosis, other (syphilis, varicella-zoster, parvovirus B19), rubella, cytomegalovirus and herpes infections

frequently require sequential imaging and therefore are preferably imaged by MRI include tuberous sclerosis, metabolic disorders and brain tumors.

Approach to intracranial calcifications and the differential diagnosis

Calcium deposits occur physiologically or in association with pathological processes (Table 1). Physiological intracranial calcification is any intracranial calcification unrelated to disease processes [8]. Physiological intracranial calcification is not an expected neuroimaging finding in the neonatal and infantile periods. As children grow older, physiological calcifications occur with increasing frequency in various areas, such as the habenula, pineal gland, choroid plexus and dura mater (Table 2) [8, 17–21]. The bilateral basal ganglia, particularly the globus pallidum, are the most common site for physiological intracranial parenchymal calcification, more frequently in older children, particularly after 13–15 years of age [22]. Causes of pathological intracranial calcification are varied and can be further divided into infectious, congenital, endocrine/metabolic, vascular and neoplastic etiologies (Table 1).

Table 2 Location, general information and typical neuroimaging characteristics of physiological intracranial calcifications and suspicious intracranial calcifications

Location	General information	Typical neuroimaging characteristics	Suspicious neuroimaging characteristics
Habenula	Epithalamic structure Paired small nuclei adjacent to the 3rd ventricle, rostral to the posterior commissure [8] Regulation of the limbic system [18]	Absent in younger than 3 years Calcifications found in 15% of the adults [8] Present in 10% of children younger than 10 years [18] Typically small and curvilinear [8]	Calcifications reported more common in schizophrenia [8]
Pineal gland	Epithalamic structure in the quadrigeminal cistern [19] Nighttime secretion of melatonin [18]	Absent in younger than 3 years Found in 1% younger than 6 years Found in 5% age 0–9 years [18] Single or punctate in 71% Large/more numerous in 29% [18]	Early onset, large and extensive calcifications considered suspicious, granting a thorough clinical and biochemical assessment Serial neuroimaging to exclude the early presentation of a pineal gland tumor [18]
Choroid plexus	In the ventricular system Cuboidal epithelial cells, vessels and connective tissue Cerebrospinal fluid production, filtering and absorption [18, 20]	Calcifications commonly found in the choroid plexus glomus within the atria of the lateral ventricles [18] Found in 12% of children [18] Small amount of calcification in lateral ventricles considered physiological at any age [18]	Large and bulky; calcification occurring outside the choroid plexus glomus considered suspicious in children younger than 10 years [18]
Dura mater	Thickest of all meningeal membranes [21] Mechanical support and neurovascular conduit [18] Falx cerebri, tentorium, tentorial incisura, falx cerebelli, and *diaphragma sellae*	Calcifications uncommon in children [18, 20] Found in 1% of cases (exclusively in the tentorium and falx cerebri) Common in patients with previous craniotomies [18]	Extensive dura mater calcifications in young patients should raise suspicion for pathological conditions, including basal cell nevus syndrome, meningiomas, sequelae of prior subdural or epidural hemorrhage, and calcium/phosphate imbalance

Neonatal 0 to 3 months	Infants 4 months to 2 years	Early childhood 3 to 8 years old	Middle childhood 9 to 11 years old	Adolescence
CMV	HIV	Pineal gland	Habenula	Carbonic anhydrase
Toxoplasmosis	Cockayne syndrome	Choroid plexus	MELAS	Germ cell tumors
Zika virus	Aicardi-Goutières syndrome	Down syndrome	Kearns-Sayre syndrome	
Rubella	Krabbe disease	Cockayne syndrome		
Herpes	ATRT	Medulloblastoma		
Congenital lymphocytic choriomeningitis	Choroid plexus neoplasm	Ependymoma		
Varicella	COL4A1 / COL4A2	Craniopharyngioma		
Pseudo-TORCH syndrome		Choroid plexus neoplasm		

Fig. 4 Chart shows typical causes of physiological and pathological intracranial calcifications across age groups from the neonatal period to adolescence. Note that there might be some variations and overlap between the etiologies in these age groups. *ATRT* atypical teratoid rhabdoid tumor, *CMV* cytomegalovirus, *HIV* human immunodeficiency virus, *MELAS* mitochondrial myopathy, encephalopathy, lactic acidosis and stroke-like episodes, *TORCH* toxoplasmosis, other (syphilis, varicella-zoster, parvovirus B19), rubella, cytomegalovirus and herpes infections

Arriving at a definitive diagnosis in childhood intracranial calcification is not always straightforward. Age at presentation, location and additional neuroimaging findings are crucial pieces of supporting information for narrowing the differential diagnosis. Causes of intracranial calcification vary according to age group. The different etiologies of physiological and pathological intracranial calcification (in their most typical presentations) across age groups are summarized in Fig. 4. The numerous causes of intracranial calcification can alternatively be categorized into five main anatomical regions: midsagittal (Fig. 5); deep gray matter structures (involving the basal ganglia and thalami) (Fig. 6); lobar (cortical and subcortical) and ventricular (foramen of Monro, periventricular

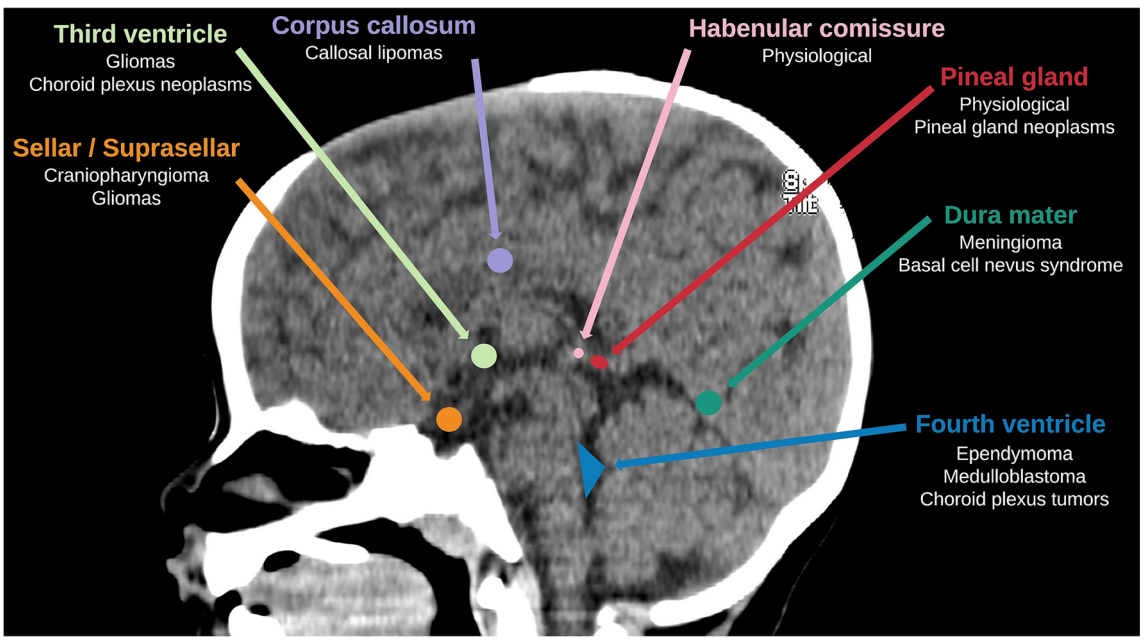

Fig. 5 Common causes of midsagittal calcifications in children arising from the sellar/suprasellar region, 3rd ventricle, corpus callosum, habenular commissure, pineal gland, dura mater of the falx and tentorium and 4th ventricle

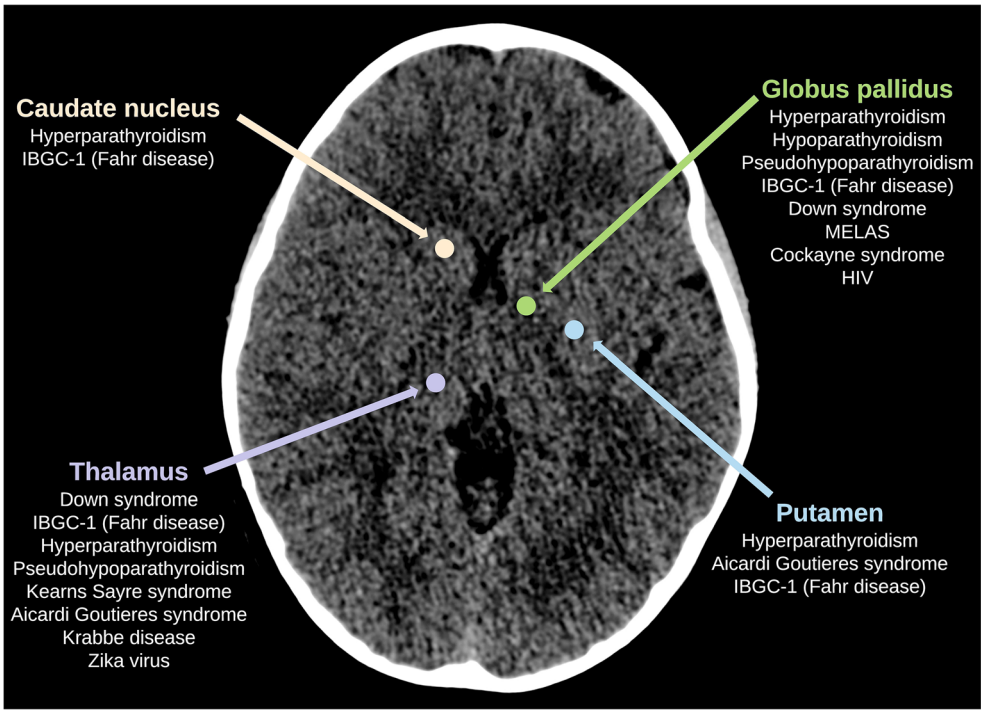

Fig. 6 Common causes of calcification arising from deep gray matter structures (thalami and basal ganglia). *HIV* human immunodeficiency virus, *IBGC-1* idiopathic basal ganglia calcification 1, *MELAS* mitochondrial myopathy, encephalopathy, lactic acidosis and stroke-like episodes

and intraventricular) (Figs. 7 and 8); and posterior fossa (Fig. 9). Common and uncommon causes of brain calcifications based on location are presented in Table 3.

A supplementary approach to the differential diagnosis of intracranial calcification might start with the following question: Is the intracranial calcification isolated or associated with other neuroimaging or clinical findings? Isolated basal ganglia calcification is typically secondary to parathyroid or thyroid dysfunction. Children with Down syndrome or human immunodeficiency virus (HIV) might also present with

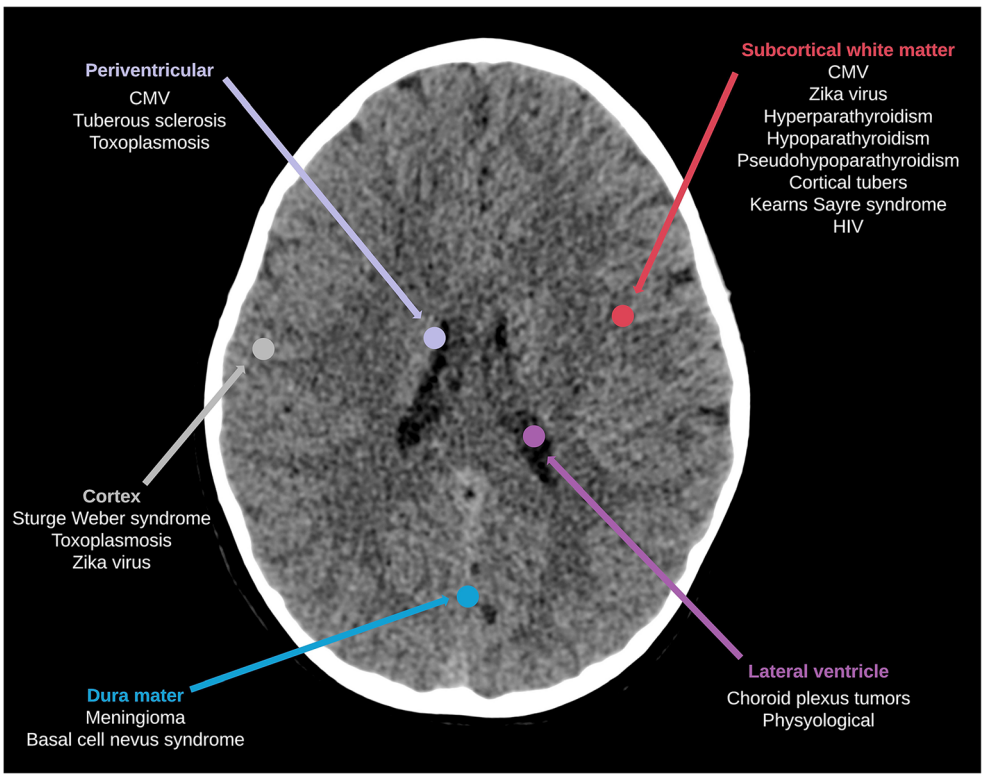

Fig. 7 Common causes of supratentorial hemispheric calcification arising from the brain parenchyma, periventricular and intraventricular structures. *CMV* cytomegalovirus, *HIV* human immunodeficiency virus

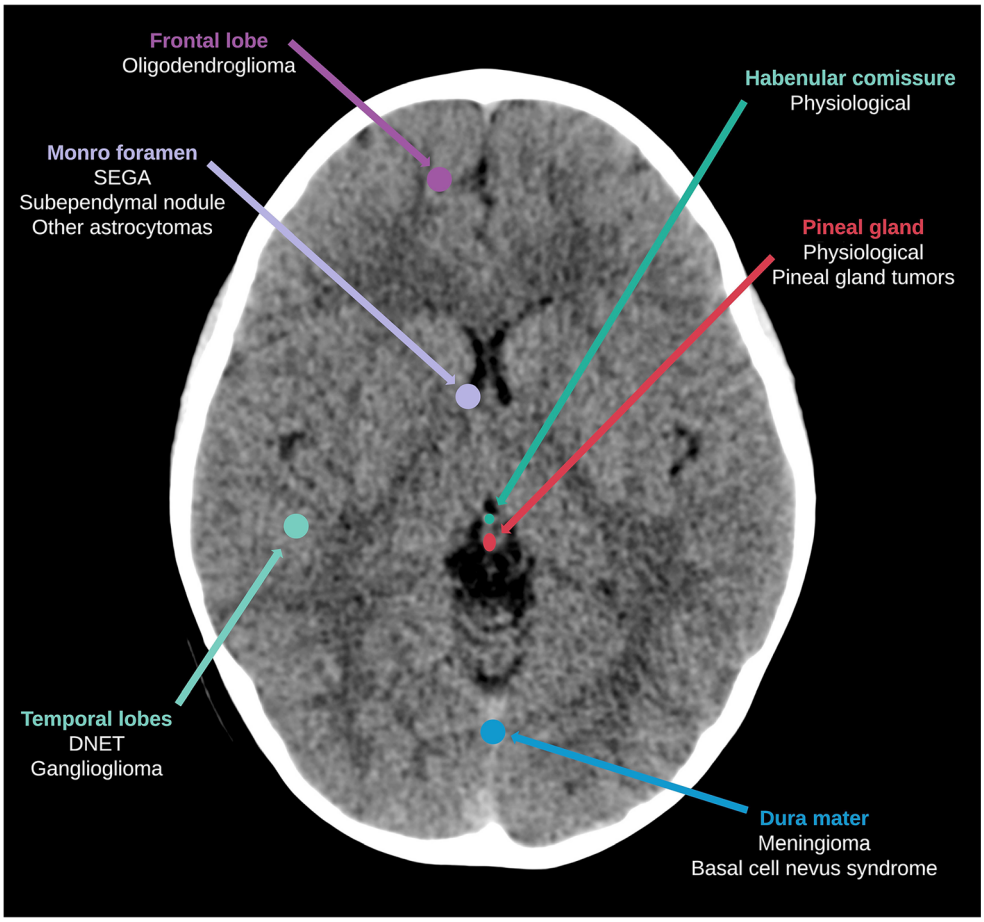

Fig. 8 Other common causes of supratentorial hemispheric calcification arising from the parenchymal, periventricular and intraventricular structures. *DNET* dysembryoplastic neuroepithelial tumor, *SEGA* subependymal giant cell astrocytoma

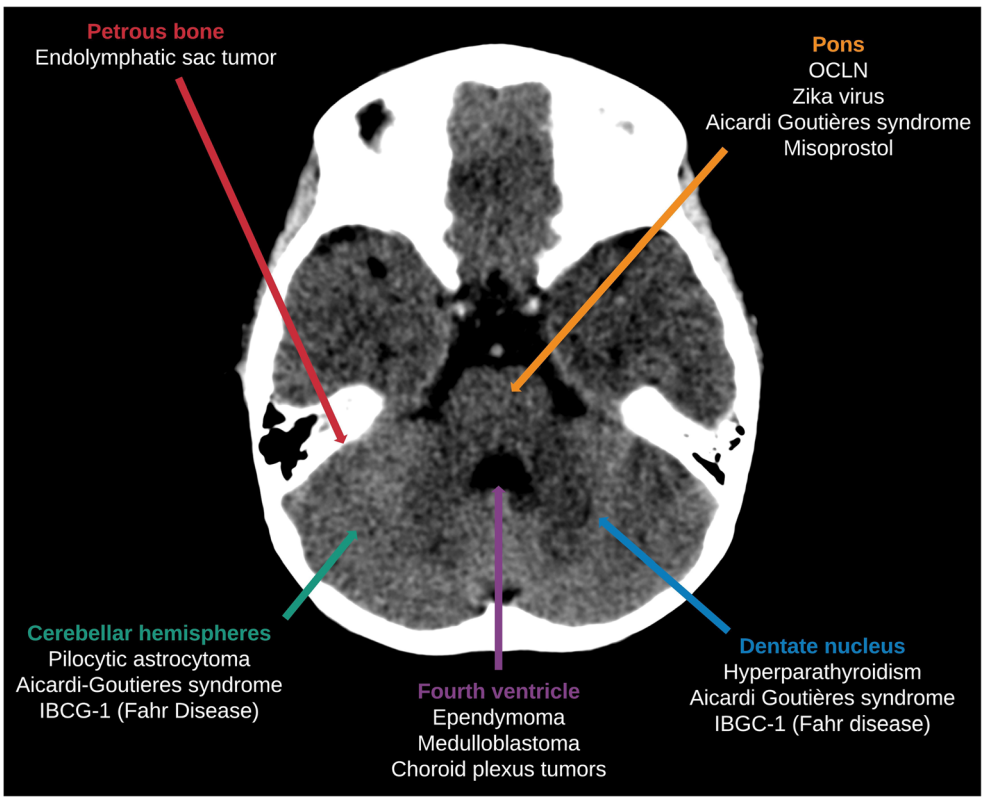

Fig. 9 Common causes of calcification arising from the posterior fossa structures. *IBGC-1* idiopathic basal ganglia calcification 1, *OCLN* occludin

Table 3 Differential diagnosis of common and uncommon causes of brain calcifications based on location[a]

Supratentorial

Globus pallidus
- Down syndrome
- Hyperparathyroidism
- Hypoparathyroidism
- Pseudohypoparathyroidism
- Hypothyroidism
- IBGC-1 (Fahr)
- Aicardi–Goutières syndrome
- HIV
- MELAS
- Kearns–Sayre syndrome
- Cockayne syndrome
- Molybdenum cofactor deficiency A
- Sulfite oxidase deficiency
- Spondyloenchondrodysplasia
- Fabry disease
- Cystic leukoencephalopathy without megalencephaly
- Nasu–Hakola disease
- Coats plus disease
- Hyperphenylalaninemia
- Spastic paraplegia-56
- Oculodentodigital dysplasia
- Spondyloenchondrodysplasia
- Rajab interstitial lung disease with brain calcifications
- Diencephalic–mesencephalic junction dysplasia syndrome-1
- Carbonic anhydrase II
- Primrose syndrome
- Early infantile epileptic encephalopathy-49
- Biotinidase deficiency
- Folate malabsorption
- Proteasome-associated autoinflammatory syndrome
- Xeroderma pigmentosum
- Haw River syndrome
- Kenny–Caffey syndrome, Type 2
- Fibrodysplasia ossificans progressiva
- Fried syndrome/Pettigrew syndrome

Putamen
- Hyperparathyroidism
- Hypoparathyroidism
- Pseudohypoparathyroidism
- Hypothyroidism
- IBGC-1 (Fahr)
- Aicardi–Goutières syndrome
- MELAS
- Kearns–Sayre syndrome
- Molybdenum cofactor deficiency A
- Sulfite oxidase deficiency
- Spondyloenchondrodysplasia
- Leukoencephalopathy with calcifications and cysts
- Nasu–Hakola disease
- Cystic leukoencephalopathy without megalencephaly
- Coats plus disease
- Hyperphenylalaninemia
- Oculodentodigital dysplasia
- Rajab interstitial lung disease with brain calcifications
- Diencephalic–mesencephalic junction dysplasia syndrome-1
- Carbonic anhydrase II
- Primrose syndrome
- Early infantile epileptic encephalopathy-49
- Biotinidase deficiency
- Folate malabsorption
- Proteasome-associated autoinflammatory syndrome
- Xeroderma pigmentosum
- Haw River syndrome
- Kenny-Caffey syndrome, Type 2
- Fibrodysplasia ossificans progressiva
- Fried syndrome/Pettigrew syndrome

Caudate nucleus
- Hyperparathyroidism
- Hypoparathyroidism
- Pseudohypoparathyroidism
- Hypothyroidism
- Aicardi–Goutières syndrome
- IBGC-1 (Fahr)
- Toxoplasmosis
- MELAS
- Kearns–Sayre syndrome
- Cockayne syndrome
- Molybdenum cofactor deficiency A
- Sulfite oxidase deficiency
- Cystic leukoencephalopathy without megalencephaly
- Nasu–Hakola disease
- Coats plus disease
- Hyperphenylalaninemia
- Oculodentodigital dysplasia
- Spondyloenchondrodysplasia
- Rajab interstitial lung disease with brain calcifications
- Diencephalic–mesencephalic junction dysplasia syndrome-1
- Carbonic anhydrase II
- Primrose syndrome
- Early infantile epileptic encephalopathy-49
- Biotinidase deficiency
- Folate malabsorption
- Proteasome-associated autoinflammatory syndrome
- Xeroderma pigmentosum
- Haw River syndrome
- Kenny–Caffey syndrome, Type 2
- Fibrodysplasia ossificans progressiva
- Fried syndrome/Pettigrew syndrome

Thalamus
- Down syndrome
- Hyperparathyroidism
- Hypoparathyroidism
- Pseudohypoparathyroidism
- IBGC-1 (Fahr)
- Aicardi–Goutières syndrome
- Krabbe disease
- Zika virus
- MELAS
- Kearns–Sayre syndrome
- Cockayne syndrome
- Molybdenum cofactor deficiency A
- Sulfite oxidase deficiency
- Fabry disease
- Carbonic anhydrase deficiency Type 2
- Cystic leukoencephalopathy without megalencephaly
- Coats plus disease
- Pseudo-TORCH syndrome-1
- Hyperphenylalaninemia
- Rajab interstitial lung disease with brain calcifications
- Diencephalic–mesencephalic junction dysplasia syndrome-1
- Carbonic anhydrase II
- Folate malabsorption
- Proteasome-associated autoinflammatory syndrome
- Haw River syndrome

Lobar
- DNET
- Ganglioglioma
- Pilocytic astrocytoma
- Post-ischemic
- Ependymoma
- Oligodendroglioma

Cortical
- Tuberous sclerosis (tubers)
- Post-ischemic
- Sturge–Weber syndrome
- Toxoplasmosis
- Zika virus
- CMV
- Cockayne syndrome
- Coats plus disease
- IBGC-1
- Brain small vessel disease-1 with or without ocular anomalies

Subcortical
- Cavernous malformation
- Sturge–Weber syndrome
- CMV
- Tuberous sclerosis (tubers)
- HIV
- Zika virus
- Hyperparathyroidism
- Hypoparathyroidism
- Pseudohypoparathyroidism
- Hypothyroidism
- Post-ischemic
- Kearns–Sayre syndrome

Periventricular
- CMV
- Tuberous sclerosis (subependymal nodules)
- Toxoplasmosis
- Zika virus
- Post-ventriculitis
- Rubella
- Aicardi–Goutières syndrome
- COL4A1
- Juvenile Alexander disease
- X-linked adrenoleukodystrophy
- Pseudo-TORCH Syndrome 2

Table 3 (continued)

	- Brain small vessel disease-2 - Raine syndrome - Xeroderma pigmentosum	- USP18 - Aicardi–Goutières syndrome - IBGC-1 - SCN3A - Cystic leukoencephalopathy without megalencephaly - Coats plus disease - Pseudo-TORCH syndrome-1 - Pseudo-TORCH syndrome-2 - Brain small vessel disease-1 with or without ocular anomalies - Brain small vessel disease-2 - Raine syndrome - Spondyloenchondrodysplasia - Diencephalic–mesencephalic junction dysplasia syndrome-1 - Carbonic anhydrase II - Phenylketonuria - Keutel syndrome	- Hemorrhagic destruction of the brain, subependymal calcification, and cataracts - Brain small vessel disease-1 with or without ocular anomalies - Brain small vessel disease-2 - Raine syndrome - Brain abnormalities, neurodegeneration, and dysosteosclerosis - Early infantile epileptic encephalopathy-49
Intraventricular - Physiological - Choroid plexus tumors - Meningioma - Tuberous sclerosis (SEGA) - Neurofibromatosis 2 - Gliomas - Central neurocytoma	**Suprasellar** - Craniopharyngioma - Astrocytomas - Lipomas	**Pineal gland** - Physiological - Pineal gland tumors - Meningioma - Choroid plexus tumors	**Habenula** - Physiological
Infratentorial			
Dentate nucleus region - Hyperparathyroidism - Aicardi–Goutières syndrome - IBGC-1 (Fahr) - Cockayne syndrome - Pseudo-TORCH syndrome-1 - Coats plus disease - Oculodentodigital dysplasia - Kenny–Caffey syndrome, Type 2 - Fibrodysplasia ossificans progressiva	**Cerebellum** - Medulloblastoma - Pilocytic astrocytoma - Hyperparathyroidism - Pseudo-TORCH syndrome-1 - Aicardi–Goutières syndrome - IBGC-1 - Nasu–Hakola disease - Kenny–Caffey syndrome, Type 2	**Brainstem** - CMV - Zika virus - Aicardi–Goutières syndrome - Pseudo-TORCH syndrome-1 - Misoprostol - Coats plus disease	**4th ventricular** - Ependymoma - Medulloblastoma - Gliomas - Choroid plexus tumors	**Dura mater** - Basal cell nevus syndrome - Meningioma - Post-hemorrhagic - Papillon–Lefèvre syndrome - Brachyolmia Type 2 - Marshall syndrome

CMV cytomegalovirus, *DNET* dysembryoplastic neuroepithelial tumor, *HIV* human immunodeficiency virus, *IBGC-1* idiopathic basal ganglia calcification-1, *MELAS* mitochondrial myopathy, encephalopathy, lactic acidosis and stroke-like episodes, *SEGA* subependymal giant cell atrocytoma, *TORCH* toxoplasmosis, other (syphilis, varicella-zoster, parvovirus B19), rubella, cytomegalovirus and herpes

[a] Note that there is overlap between causes of calcification in different locations, and many broad etiologies; for example, post-ischemic calcification can occur in multiple regions

isolated basal ganglia calcification. Additional neuroimaging findings, including the presence of cortical malformations, clastic changes, vascular malformation, mass effect, cortical changes and skin lesions, must be considered to narrow the differential diagnosis (Fig. 10).

Physiological intracranial calcifications

Habenula

The habenula is a paired paramedian dorsal epithalamic gray-matter structure located just anterior/superior to the pineal

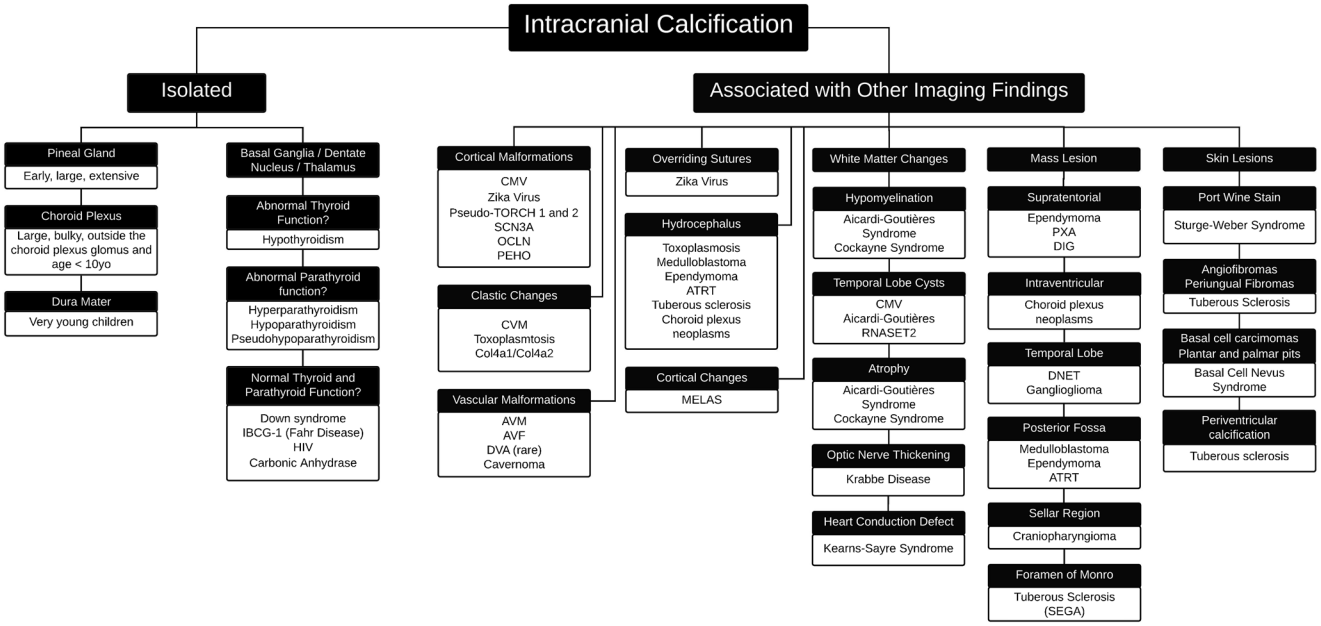

Fig. 10 An approach to intracranial calcification identified on diagnostic imaging in children based on the absence or presence of additional neuroimaging and clinical findings. *ATRT* atypical teratoid rhabdoid tumor, *AVF* arteriovenous fistula, *AVM* arteriovenous malformation, *CMV* cytomegalovirus, *DIG* desmoplastic infantile ganglioglioma, *DNET* dysembryoplastic neuroepithelial tumor, *DVA* developmental venous anomaly, *HIV* human immunodeficiency virus, *IBGC-1* idiopathic basal ganglia calcification 1, *MELAS* mitochondrial myopathy, encephalopathy, lactic acidosis and stroke-like episodes, *PEHO* progressive encephalopathy with edema, hypsarrhythmia and optic atrophy, *PXA* pleomorphic xanthoastrocytoma, *SEGA* subependymal giant cell astrocytoma, *TORCH* toxoplasmosis, other (syphilis, varicella-zoster, parvovirus B19), rubella, cytomegalovirus and herpes infections

gland, and it can be difficult to distinguish on axial images. The habenula is involved in various complex functions, mainly in regulating the limbic system (Fig. 11) [18]. In a study by Whitehead et al. [18], habenular calcifications were identified in only 10% of children younger than 10 years and were absent in children younger than 2 years.

Pineal gland

The pineal gland is a small lobular midline epithalamic structure in the quadrigeminal cistern between the habenular and posterior commissures. The pineal gland's primary function is the nighttime secretion of melatonin (Fig. 11) [19]. Histological studies have indicated that pineal gland calcification starts early in life and progresses with age [23]. Whitehead et al. [18] found a 5% prevalence of pineal calcification in CT examinations of 500 children ranging from 0 to 9 years of age. Pineal calcification is uncommon before 6 years of age, only found in 1% of cases and absent in children younger than 3 years. Pineal calcifications can be single or punctate (71%), numerous or larger (29%) [18]. Therefore, early onset large and extensive pineal calcifications should be considered with suspicion, prompting a thorough clinical and biochemical assessment. Serial neuroimaging should also be a consideration for excluding an early presentation of a pineal tumor (Fig. 12) [18].

Choroid plexus

The choroid plexus is a secretory tissue primarily involved in the production of cerebrospinal fluid [21]. Physiological choroid plexus calcifications are more common in the choroid plexus glomus within the atria of the lateral ventricles (Fig. 11) [22]. Premature pathological choroid plexus calcification can occur following ventriculitis or intraventricular hemorrhage. Whitehead et al. [18] found a 12% prevalence of choroid plexus calcification in their cohort. These calcifications can occur in all age groups (including early childhood), might be uni- or bilateral, and are typically punctate and few. Small calcifications might be seen in the choroid plexus at the foramina of Luschka in older children. Large and bulky calcifications occurring outside the choroid plexus glomus should be regarded with suspicion in children younger than 10 years (Fig. 13) [18].

Dura mater

The dura is the thickest of the meningeal membranes [21] and serves as mechanical support for the intracranial structures and as a neurovascular conduit [18]. Physiological dura mater calcification increases in frequency with increasing age and is particularly common among the older adults. Dural calcifications are uncommon in children [18, 20]. In the Whitehead et al. [18] cohort, dural calcifications were found only in 1%

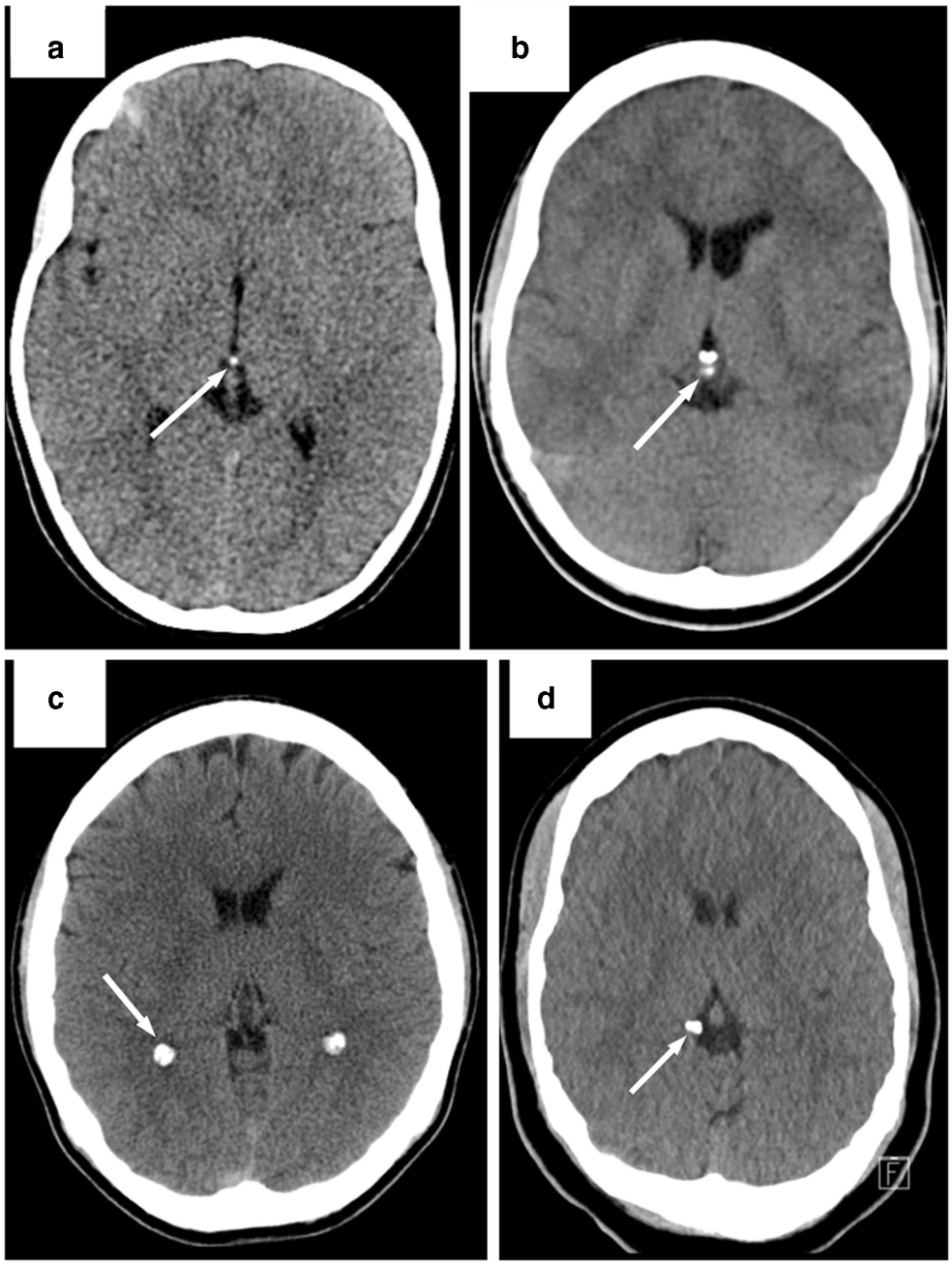

Fig. 11 Physiological intracranial calcification in four children on nonenhanced axial CT images. **a** Punctate calcification in the habenula (*arrow*) in a 5-year-old boy. **b** Small pineal calcification (*arrow*) located immediately posterior to habenular calcification in a 13-year-old girl. **c** Bilateral choroid plexus calcification (*arrow*) in a 12-year-old girl. **d** Nodular dura mater calcification along the tentorial incisura on the right side (*arrow*) in a 16-year-old girl

of cases, more commonly in the tentorium and falx cerebri, and particularly in children who underwent previous craniotomies (Fig. 11) [18]. Punctate and isolated calcifications are typically of no clinical significance [25]. Extensive dural calcifications in young patients should raise suspicion for pathological conditions such as basal cell nevus syndrome, meningiomas, sequelae of prior subdural or epidural hemorrhage, and calcium/phosphate imbalance [26].

The walls and membranes in chronic subdural and epidural hematomas and intracranial collections can also calcify or eventually ossify. Calcification or ossification is a rare chronic complication of subdural hematomas that is more frequently found in children and young adults than in older adults, occurring in 0.3% to 2.7% of patients with chronic subdural hematoma [27].

Basal ganglia

Overall, basal ganglia calcification is an uncommon finding, particularly in the younger pediatric population, and is more frequent with aging. In pediatric neurology practice, the presence of basal ganglia calcification is considered suspicious

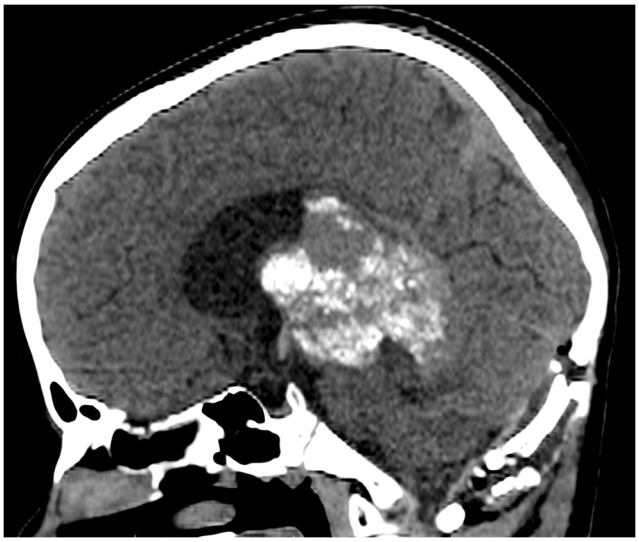

Fig. 12 Nonenhanced CT sagittal reconstructed image in a 7-year-old boy with pineoblastoma. Note the large hyperdense lobulated mass with multiple calcified foci compressing the cerebral aqueduct and causing supratentorial hydrocephalus

and commonly triggers the investigation of a possible neurologic disorder.

In a study performed in 1,569 people (age range 15–85 years) who had brain CT for head trauma and no evidence of pathological findings, basal ganglia calcification was found in 0.8% of the examinations. In this study, no one younger than 25 years had basal ganglia calcification; these calcifications were more frequent in adults older than 65 [28].

A review of CT examinations of 7,081 patients (age range 5–84 years) demonstrated basal ganglia calcification in 53 of them, 75% of these older than 50 years [29]. Only 6 people with basal ganglia calcification were younger than 20 years, and 4 of these had a history of radiation therapy [29]. Most of the patients older than 50 years had no identifiable condition to explain the presence of basal ganglia calcification [29]. In an extensive retrospective review of brain CT reports in 18,000 children (0–15 years of age) by Kendall and Cavanagh [20], pathological intracranial calcification was recorded in 1.6% (290). In 15% (43) of these, diffuse basal ganglia calcification was noted, although it bore little relation to the diverse clinical symptomatology, and routine biochemical studies showed a disorder of metabolism to be present in only 6 cases.

In another study, performed in 4,383 children who underwent 6,428 CT scans, basal ganglia calcification was detected in approximately 1.1% of the children, with a mean age of 5.3 years (range 0.5–20 years) [30]. Among the 48 children who had basal ganglia calcification, 16 (33%) had been diagnosed with cancer, 14 (29%) had tuberous sclerosis or congenital infection, and 18 (38%) had other medical conditions. All patients with cancer had been treated with radiation therapy to the diencephalon, and calcifications first became apparent at a median of 10 months after treatment. Other medical conditions included neonatal asphyxia in 3; metabolic disease in 3 — including Kearns–Sayre syndrome, MELAS (mitochondrial myopathy, encephalopathy, lactic acidosis and stroke-like episodes) and Krabbe disease; congenital

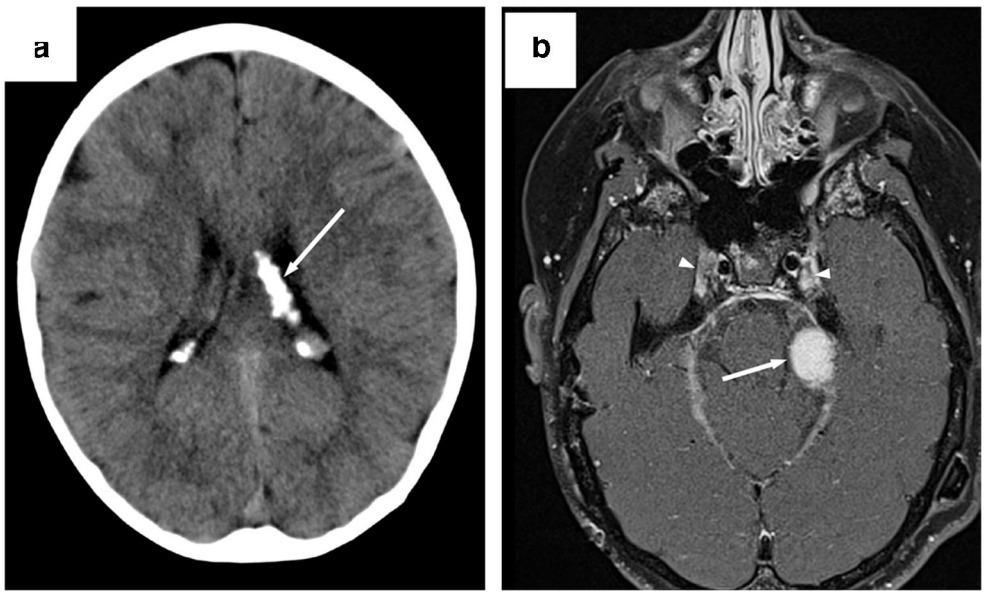

Fig. 13 Choroid plexus hypertrophy in a 12-year-old girl with neurofibromatosis Type 2. **a** Nonenhanced axial CT image at the level of the lateral ventricle bodies shows chunky calcification in the choroid plexus in the left lateral ventricle (*arrow*). Calcification of the choroid plexus is rather common in neurofibromatosis Type 2, usually unrelated to meningiomas. Intraventricular meningiomas are typically large soft-tissue enhancing lesions that might show foci of calcification. **b** Axial enhanced fat-saturated T1-weighted MR image shows enhancing trigeminal nerve Schwannomas in both Meckel caves (*arrowheads*) and a meningioma along the left tentorial incisura (*arrow*)

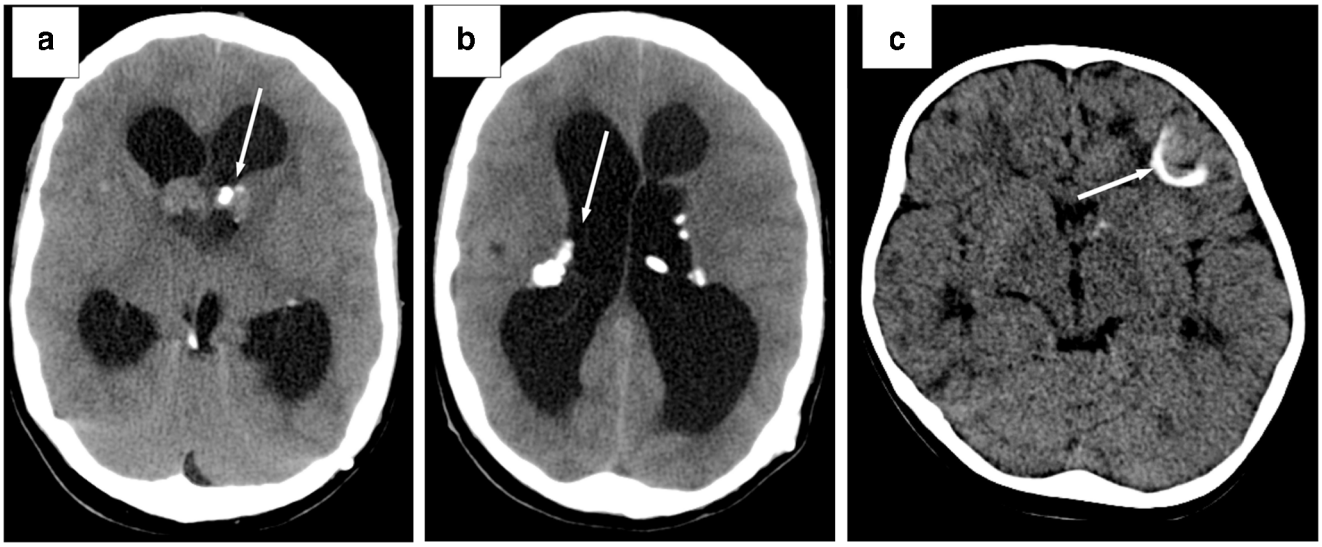

Fig. 14 Nonenhanced CT axial images of two children with tuberous sclerosis. **a**, **b** CT in a 15-year-old girl with bilateral subependymal giant cell astrocytomas shows internal calcification on the left (*arrow* in **a**) and multiple bilateral calcified subependymal nodules (*arrow* in **b**). It is unclear whether the calcification is caused by engulfing of a calcified subependymal nodule by the tumor. **c** Nonenhanced axial CT in a 2-year-old boy shows calcification within a tuber (*arrow*)

anomalies; meningitis; Fahr disease; and others [30]. Neurologic symptoms were common in children of all groups but could not be correlated to basal ganglia calcification changes. Calcium and phosphorus metabolism was evaluated in 19 patients and was abnormal in 1. Based on this extensive study, basal ganglia calcification in childhood occurs primarily as a consequence of cancer treatment or in those with generalized neurologic dysfunction [30].

Congenital causes of intracranial calcifications

Congenital syndromic causes of intracranial calcification (which might be present at birth or develop subsequently) comprise a broad group of entities, mostly made up of neurocutaneous syndromes (phakomatosis) and Down syndrome.

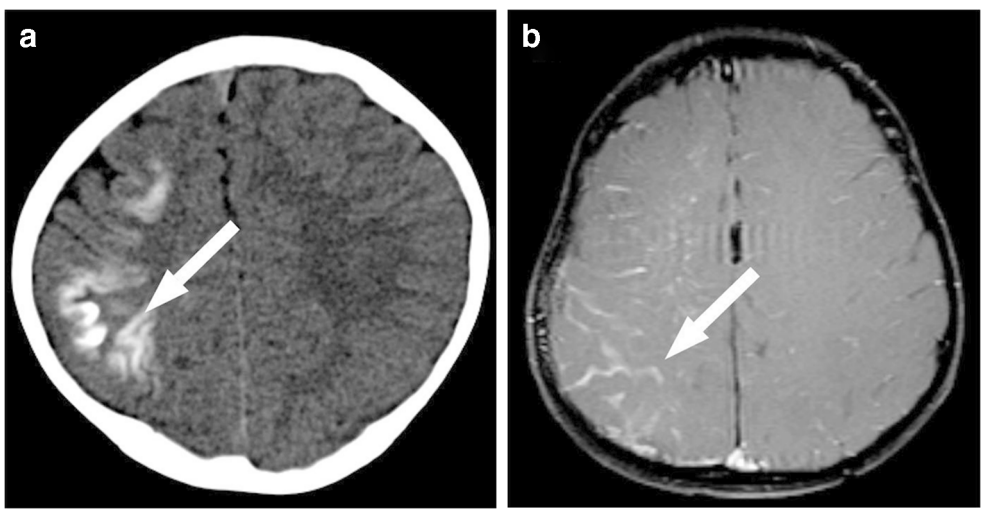

Fig. 15 Imaging in a 3-year-old boy with Sturge–Weber syndrome and a port-wine stain over the right eye. **a** Nonenhanced CT axial image shows cortical tram-track calcification about the gyri in the right parietal and frontal lobe (*arrow*), with prominent sulci from atrophy. **b** Axial fat-saturated nonenhanced T1-weighted MR image shows pial/meningeal angiomatosis and enlarged deep medullary veins involving the right cerebral hemisphere and in the right centrum semiovale (*arrow*)

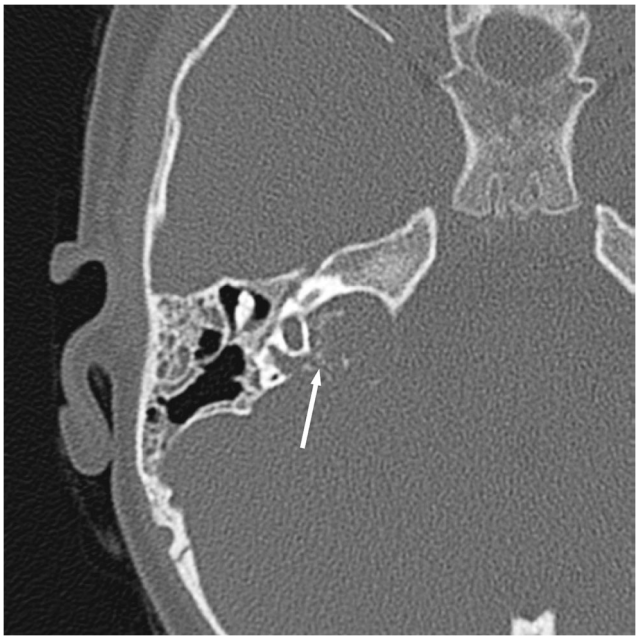

Fig. 16 Endolymphatic sac tumor in a 5-year-old girl with von Hippel–Lindau syndrome. Nonenhanced CT axial image shows a large, expansile lytic lesion in the right temporal bone extending along the posterior margin of the petrous portion, with multiple punctate foci of calcification (*arrow*), at least some of which are sequestered bone. The tumor involved the internal auditory canal, vestibular aqueduct and endolymphatic sac

Neurocutaneous syndromes

Neurocutaneous syndromes are a highly heterogeneous group of congenital disorders with a variable degree of penetration, primarily involving structures derived from the neuroectoderm. In addition to the central nervous system (CNS), these syndromes can involve the peripheral nerves, skin, eye and other systems [31]. The most common phakomatoses associated with intracranial calcification are tuberous sclerosis complex, Sturge–Weber syndrome, von Hippel–Lindau syndrome, and basal cell nevus syndrome.

Tuberous sclerosis complex

Tuberous sclerosis complex is caused by mutations in the *TSC1* (OMIM #191100) or *TSC2* (OMIM #613254) genes leading to hamartin or tuberin function abnormalities, respectively [32]. According to the International Tuberous Sclerosis Complex Consensus Group, the diagnosis can be made by the presence of typical skin lesions, seizures and cellular overgrowth or hamartomas in the heart, lungs, brain and kidneys [33, 34]. Neuroimaging findings include cortical tubers, cortical dysplasia, subependymal nodules and subependymal giant cell astrocytoma [35]. Calcification is found in 88–93% of subependymal nodules (Fig. 14) [36–38], which are usually not calcified at birth but become more evident with increased age [39, 40]. Rarely, subependymal nodules are calcified very early in the disease, including in the neonatal period. Calcification occurs in 43–62% of tubers [39, 41, 42], which typically do not grow over time, staying proportional to other parts of the growing brain in children. Although it is known that subependymal giant cell astrocytomas grow over time, there is scarce evidence in the literature assessing the progression of intratumoral calcification in subependymal giant cell astrocytomas. Nevertheless, a subependymal giant cell astrocytoma can engulf a nearby calcified subependymal nodule. Retinal hamartomas, which can also calcify, are present in 40–

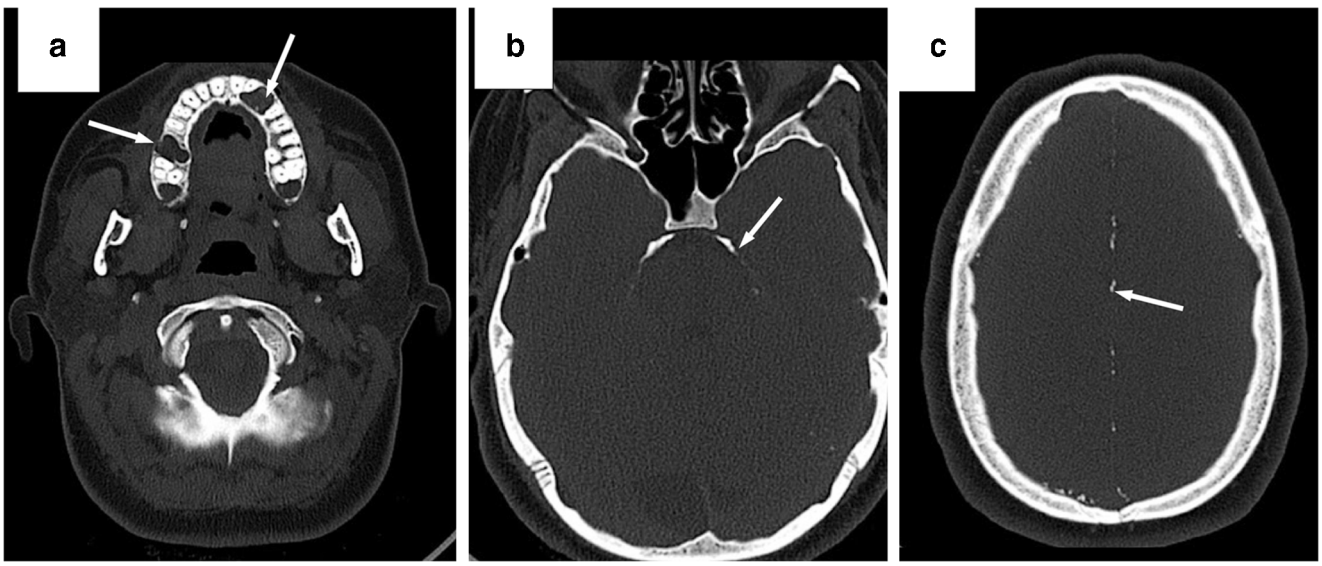

Fig. 17 Nonenhanced axial CT images in a 14-year-old girl with basal cell nevus syndrome show (**a**) bilateral maxillary odontogenic cysts (*arrows*), (**b**) thick and linear dural calcification in the petroclinoid ligaments (*arrow*) and (**c**) multiple punctate calcium deposits along the falx (*arrow*)

Fig. 18 Nonenhanced axial CT in an 11-year-old boy with Down syndrome with new onset of seizures shows bilateral asymmetrical pallidal calcification, more prominent on the left side (*arrows*)

50% of these patients [43]. Retinal hamartomas might be further characterized as flat and translucent, nodular or transitional. Calcifications do not typically occur in the flat lesions and might be present in 50% of the nodular type [44].

Sturge–Weber syndrome

Sturge–Weber syndrome (OMIM #185300) is a non-hereditary disease recently linked to a somatic mutation in the *GNAQ* gene [45]. Sturge–Weber syndrome is characterized by multiple angiomas involving the face, with the typical port-wine stain; in the choroid of the eye, associated with glaucoma; and in the leptomeninges, associated with leptomeningeal angiomatosis [46]. Seizures are the most common neurologic manifestation, typically present in the first months after birth [45, 47]. Neuroimaging findings include prominent transmedullary veins, enlarged choroid plexus, and leptomeningeal angiomatosis (leptomeningeal enhancement in the affected area). Because of abnormal venous drainage, the brain undergoes chronic venous congestion and ongoing chronic ischemia, leading to focal volume loss, which can be cortical and subcortical. The typical pattern of calcification in more advanced lesions is known as the tram-track calcification, typically appearing as gyriform calcifications along the superficial surface of the affected brain (Fig. 15) [48]. In addition, ipsilateral calvarial and regional sinus enlargement can be seen in response to the volume loss, which in severe cases can produce a Dyke–Davidoff–Masson appearance of the calvarium [49].

Von Hippel–Lindau syndrome

Von Hippel–Lindau syndrome (OMIM #193300) is an uncommon familial neoplastic disease caused by mutations of the *VHL* gene (a tumor suppressor gene) on Chromosome 3. Children might present with CNS and retinal hemangioblastomas, renal cysts and clear cell renal cell carcinoma, pancreatic cysts, pheochromocytoma, neuroendocrine tumors, endolymphatic sac tumors, and epididymal and broad ligament cysts [50]. CNS hemangioblastomas are the most common tumors, affecting 60–80% of all patients [51, 52] and involving the cerebellum (16–69%), brainstem (5–22%), spinal cord (13–53%), cauda equina (11%), or uncommonly supratentorial brain (1–7%) [52, 53]. Hemangioblastomas do not typically calcify. Intracranial calcifications are more commonly associated with endolymphatic sac tumors (Fig. 16),

Table 4 Neonatal and postnatal infectious causes of intracranial calcification

Neonatal infections (TORCH infections)	Postnatal infections
- Cytomegalovirus	- Neurocysticercosis
- Toxoplasmosis	- Toxoplasmosis
- Zika virus	- *Mycobacterium tuberculosis*
- Herpes (neonatal and postnatal)	- Healed cerebral abscess
- Rubella	- Post-meningitis and ventriculitis
- Varicella	- Other healed encephalitides
- Congenital lymphocytic choriomeningitis[a]	- HIV (TORCH)[b]

HIV human immunodeficiency virus, *TORCH* toxoplasmosis, other (syphilis, varicella-zoster, parvovirus B19), rubella, cytomegalovirus and herpes infections

[a] Congenital infection not included as a TORCH infection

[b] TORCH infection that causes symptoms in the postnatal period

Table 5 Neonatal infectious causes of intracranial calcification

TORCH	Pathogen	Calcification	Associated CNS findings	Additional findings
CMV	- Cytomegalovirus - dsDNA virus - Herpesviridae	- Present in 34% to 70% - Thick, chunky, fine or punctate - CT, T2* and SWI are highly sensitive - Periventricular - Basal ganglia - Brain parenchyma [60]	- Lissencephaly - Pachygyria - Polymicrogyria - Schizencephaly - White matter changes - Ventriculomegaly - Delayed myelination - Periventricular or temporal lobe cysts - Cerebral/cerebellar volume loss - Ventricular adhesions - Ventricular septations - Lenticulostriate vasculopathy [60]	- Developmental delay - SNHL - Seizures - Microcephaly - Hepatosplenomegaly - Jaundice - Thrombocytopenic purpura - Low birth weight - Petechiae - Preterm birth - Fetal growth restriction - Chorioretinitis [60, 61]
Toxoplasmosis	- Toxoplasma gondii - Intracellular protozoan	- ICC, 80% - Subtle, coarse and chunky - No ventricular predilection - Randomly distributed - Large - Periventricular - Diffuse [62]	- Hydrocephalus - Macrocephalus/microcephalus - Parenchymal destruction/volume loss - Lenticulostriate vasculopathy - Microphthalmia [63]	- Chorioretinitis - Hepatosplenomegaly - Jaundice - Seizures - Lymphadenopathy - Abnormal cerebrospinal fluid - Anemia [62]
Rubella (German measles)	- Rubella virus - ssRNA virus - Togaviridae	- Periventricular - Basal ganglia - Progressive diffuse - Thalamus [64]	- Hydranencephaly - Ventriculomegaly - Cerebellar atrophy - "Branched candlestick" on US	- Developmental delay - Multiple organs and systems - Microphthalmia - Congenital cataracts - Inner ear abnormalities - Microcephaly - Congenital heart disease - Increased risk of Type 1 diabetes in childhood [61, 65]
Herpes	- Herpes Type 1 and Type 2 - dsDNA viruses - Herpesviridae - HSV1, during birth - HSV2, accounts for 80–90% of all neonatal cases	- Thalamus - Basal ganglia - Peri-insular cortex - Periventricular white matter - Gray/white junction in infants - Progressive and diffuse [66, 67]	- Multifocal or often limited to the temporal lobes or brainstem and cerebellum - MRI more sensitive than CT - DWI is sensitive in the early infection - Encephalitis - Parenchymal destruction - Hydrocephalus [61]	- Multiorgan failure - Liver necrosis - Microcephaly - Chorioretinitis - Skin lesions - Sepsis - Cataracts - Pneumonitis - Myocarditis - Hepatosplenomegaly - Fetal growth restriction - Developmental delay [61]
Zika	- Zika virus - ssRNA viruses - Flaviviridae	- Almost universal - Frontal > parietal > occipital > temporal lobes - Punctate/coarse - Cortical/subcortical - Basal ganglia - Thalami - Brainstem - Cerebellum [61, 68]	- Cerebral volume loss - Cerebral mantle thinning - Malformation of cortical development - Ventriculomegaly - Cerebellar hypoplasia - Corpus callosum changes - Hypomyelination - Prominent occipital bone - Overriding sutures - Redundant skin [68, 69]	- Fetal brain disruption sequence - Microcephaly - Macrocephaly - Normocephaly - Craniofacial disproportion - Hearing loss - Arthrogryposis - Neuromotor abnormalities - Hypertonia - Spasticity - Macular scarring - Focal pigmentary retinal mottling - Seizures - Hematologic, hepatic or renal laboratory abnormalities not yet documented [61, 69]
Lymphocytic choriomeningitis (LCM)[a]	- LCM virus - ssRNA viruses - Arenaviridae	- Periventricular [70]	- Hydrocephalus - Intracranial hemorrhage - Malformation of cortical development - Pachygyria - Porencephalic cysts - Cerebellar hypoplasia [70]	- Hydrops - Microcephaly - Seizures - Neurodevelopmental disability - Chorioretinal lacunae - Panretinal pigment epithelium atrophy - Bilateral optic nerve dysplasia or atrophy

Table 5 (continued)

TORCH	Pathogen	Calcification	Associated CNS findings	Additional findings
				- Reduced caliber of retinal vessels - Nystagmus - Strabismus - Prenatal LCM virus infects brain parenchyma usually without detectable systemic effects [70]
Varicella-zoster (chickenpox)	- Varicella-zoster virus - dsRNA viruses - Herpesviridae	- Periventricular [70]	- Sequelae of necrotizing encephalitis - Hydrocephalus - Porencephaly - Hydranencephaly - Polymicrogyria - Focal lissencephaly - Severe microcephaly	- Polyhydramnios - Calcification in the liver, heart, colon, lungs, and kidneys - Cataracts - Chorioretinitis - Microphthalmia - Hydrops - Skin lesions - Cicatrix - Eye defects - Limb hypoplasia - Limb contractions - Fetal growth restriction - Multisystemic defects [71, 72]

CMV cytomegalovirus, *CNS* central nervous system, *CT* computed tomography, *dsDNA* double-stranded DNA, *dsRNA* double-stranded RNA, *HSV1* herpes simplex virus 1, *HSV2* herpes simplex virus 2, *ICC* intracranial calcification, *DWI* diffusion-weighted imaging, *MRI* magnetic resonance imaging, *SNHL* sensorineural hearing loss, *ssRNA* single-stranded RNA, *SWI* susceptibility-weighted imaging, *TORCH* toxoplasmosis, other (syphilis, varicella-zoster, parvovirus B19), rubella, cytomegalovirus and herpes infection, *US* ultrasonography

[a] Congenital infection not included as a TORCH infection

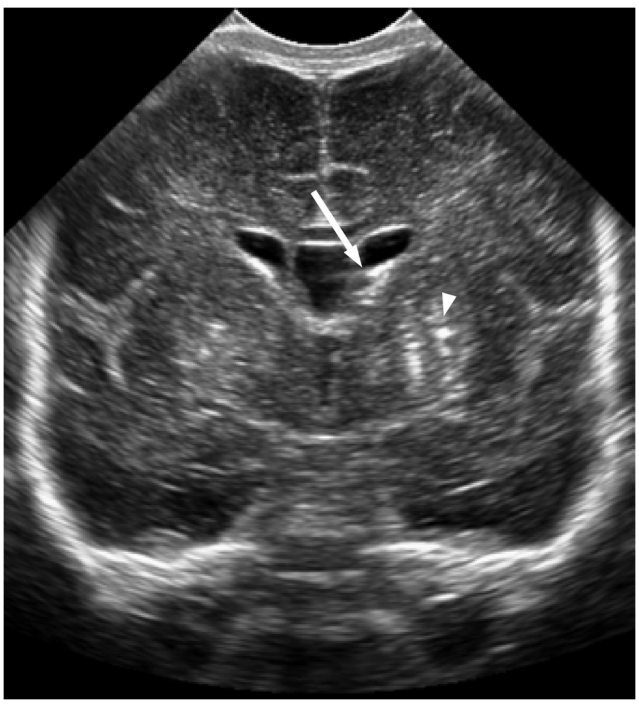

Fig. 19 Congenital cytomegalovirus infection in a 2-day-old term boy with fetal hydrops, intrauterine growth restriction, low platelets and hepatomegaly. Gray-scale ultrasonography of the brain performed through the anterior fontanelle in the coronal plane shows subependymal cyst adjacent to the left caudothalamic notch (*arrow*). Note the punctate linear branching echogenicity along the left basal ganglia in keeping with lenticulostriate vasculopathy (*arrowhead*). The ventricles are normal in size and configuration. There is no mass effect or shift of midline structures

which might demonstrate a moth-eaten appearance in the petrous temporal bone, with eventual erosive changes in the cochlea, semicircular canals, and vestibular aqueduct. Calcification might be seen within or in the periphery of endolymphatic sac tumors, often as a result of bone destruction [54].

Basal cell nevus syndrome

Basal cell nevus syndrome (OMIM #109400), or Gorlin–Goltz syndrome, is an autosomal-dominant disorder caused by a mutation in the *PTCH1* gene localized to 9q22.3 [55]. Basal cell nevus syndrome is characterized by the early development of multiple jaw keratocysts, basal cell carcinomas, ectopic dura mater calcifications, plantar and palmar pits, and abnormalities in the ocular, reproductive and skeletal systems (Fig. 17) [56]. Dura mater calcification, characteristically in the falx and tentorium, is present in more than 90% of affected individuals by age 20 years. Approximately 5% of all children with basal cell nevus syndrome develop medulloblastoma, generally the desmoplastic subtype, in the first 3 years of life [55].

Down syndrome

Down syndrome (OMIM #190685) is the most prevalent genetic disease and the most common cause of chromosomal developmental delay worldwide (Chromosome 21 trisomy)

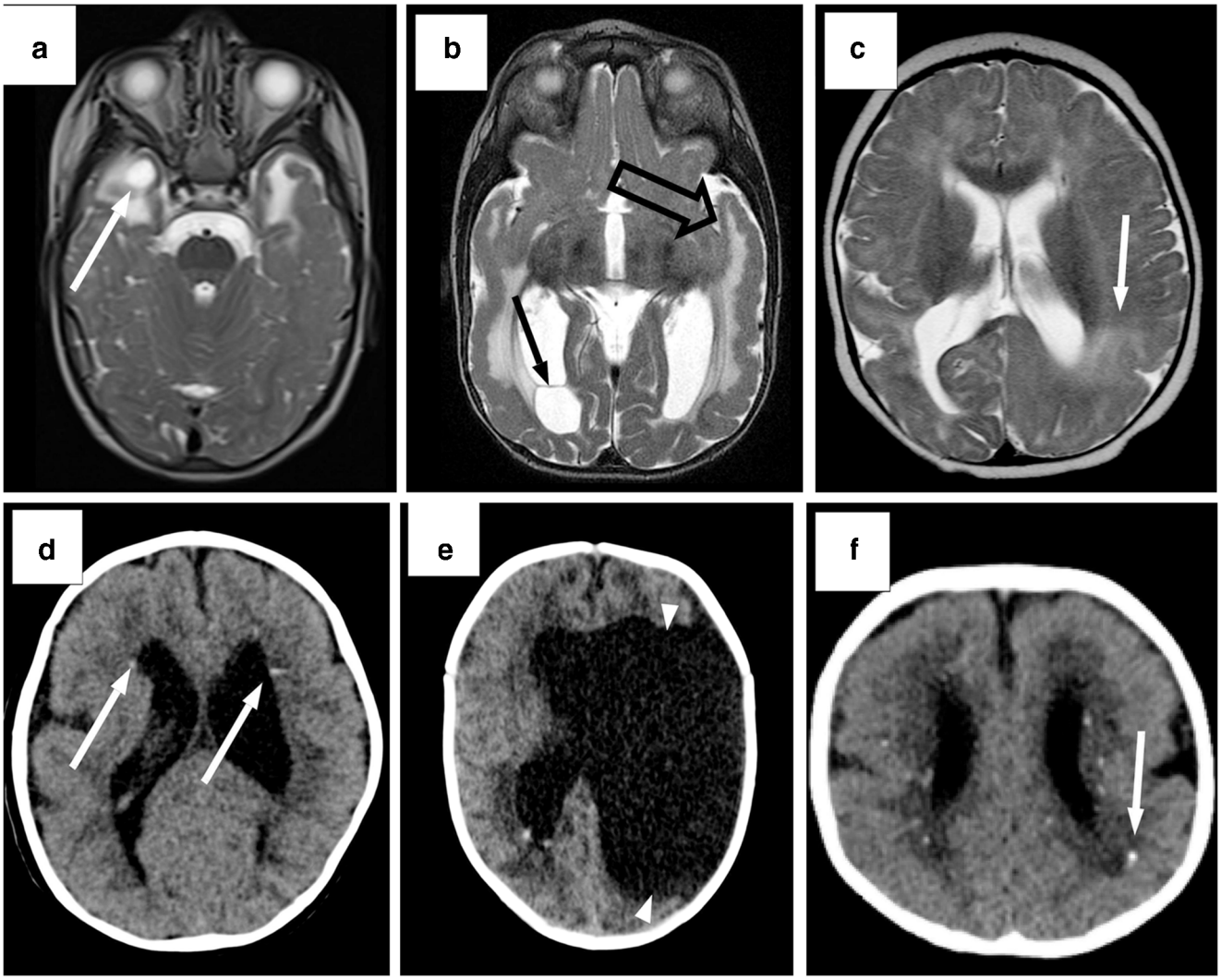

Fig. 20 CT and MRI findings in congenital cytomegalovirus infection. **a** Axial T2-weighted MR image in a 4-year-old girl shows bilateral white matter hyperintensities in both temporal poles, associated with cystic changes on the right (*arrow*). **b** Axial T2-weighted MR image in a 7-year-old boy shows bilateral white matter hyperintensities in both temporal lobes associated with perisylvian polymicrogyria (*open arrow*) and ventricular septation (*solid arrow*). **c** Axial T2-weighted MR image in a 3-year-old boy shows bilateral lateral ventricle dilatation, associated with a paucity of periventricular white matter and white matter signal changes adjacent to an area of dysplastic cortex (*arrow*). **d** Nonenhanced axial CT image in a 5-year-old girl with ventriculomegaly (*arrows*) shows periventricular calcifications. **e** Nonenhanced axial CT image in a 3-year-old girl shows a large destructive area of the brain, possibly extensive open lip schizencephaly (*arrowheads*), ventriculomegaly and punctate periventricular calcifications. **f** Nonenhanced axial CT image in a 9-year-old boy shows simplified pattern of sulcation, diffuse bilateral white matter changes, ventriculomegaly, and periventricular and subcortical calcifications (*arrow*)

[57]. Neuroimaging findings include microcephaly, cerebral atrophy (global or focal), white matter signal changes, ventriculomegaly, Dandy–Walker malformation, small posterior fossa, enlarged Sylvian fissures, skull base abnormalities (such as platybasia) and intracranial calcification [58, 59]. Intracranial calcification is present in 11–27% of cases, typically in the basal ganglia and particularly in the globus pallidus (Fig. 18) [59].

Infectious causes of intracranial calcification

Numerous infections can cause childhood intracranial calcification in both the neonatal and postnatal periods (Table 4). In the neonatal period, the most common causes are related to the TORCH complex, which includes toxoplasmosis, other (syphilis, varicella-zoster, parvovirus B19), rubella, cytomegalovirus and herpes infections (Table 5) [60–72]. The most

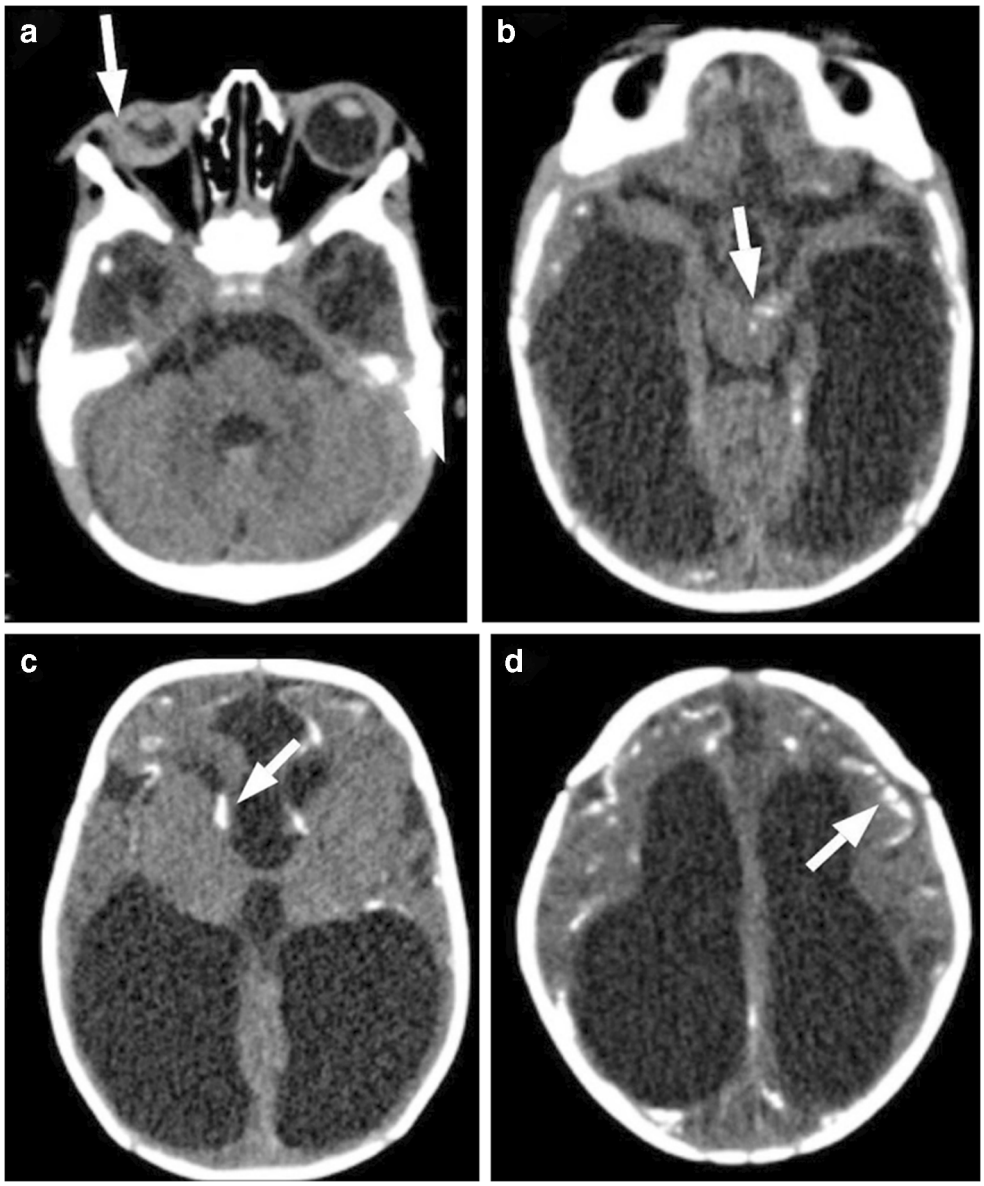

Fig. 21 Axial nonenhanced CT images in a 3-week-old full-term boy with hyperbilirubinemia and transaminitis caused by congenital toxoplasmosis infection. Note the marked diffuse ventriculomegaly, a paucity of periventricular and deep white matter and cortical mantle thinning. **a** Note the microphthalmia on the right side associated with posterior segment crescent-shape material in keeping with sequelae of necrotizing chorioretinitis (*arrow*). **b**–**d** Diffuse calcification is also evident in the brainstem (*arrow*) in (**b**) and adjacent to the caudate nuclei (*arrow*) in (**c**); there is diffuse cortical calcification (*arrow*) in (**d**)

common causes of TORCH-related intracranial calcification are cytomegalovirus and toxoplasmosis. An emerging cause of TORCH-related intracranial calcification is the Zika virus, particularly in endemic areas. Less common causes of intracranial calcification from congenital infections include herpes, rubella, varicella and congenital lymphocytic choriomeningitis. Most of the postnatal infectious intracranial calcification causes worldwide are secondary to neurocysticercosis, toxoplasmosis and tuberculosis. Other less common causes are sequelae of a cerebral abscess, meningitis, ventriculitis and other encephalitis. In some cases, TORCH-related intracranial calcification is not identified in the immediate neonatal period and is only seen later in life, such as in human immunodeficiency virus (HIV) congenital infections.

Cytomegalovirus

Cytomegalovirus is ubiquitous worldwide, with the majority of infected individuals being asymptomatic. There are two groups of people in whom cytomegalovirus can cause severe complications — the immunosuppressed and pregnant women. Intrauterine infection leading to congenital cytomegalovirus can be a major public health issue because of a high association with severe neurodevelopmental damage including microcephaly, intellectual disability, cerebral palsy and sensorineural hearing loss [60, 73]. Symptomatic congenitally infected cytomegalovirus patients almost universally demonstrate brain changes on imaging. The most common neuroimaging finding is intracranial calcification, present in 34–70% of these cases [74]. Cytomegalovirus calcification is variable,

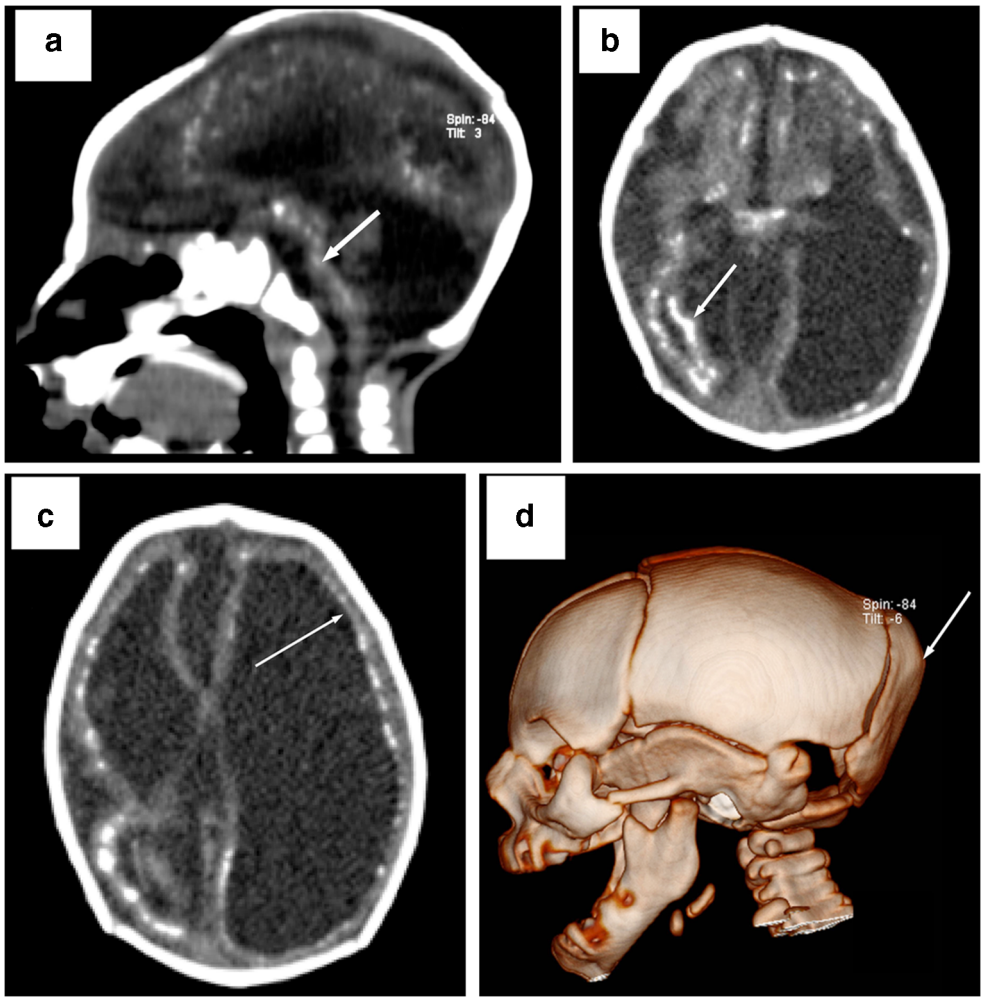

Fig. 22 Nonenhanced CT images in a 12-month-old girl with arthrogryposis, severe developmental delay and microcephaly from confirmed maternal Zika virus infection. **a** Sagittal reconstructed image shows significant microcephaly with evident craniofacial disproportion, as well as marked brainstem atrophy with calcification (*arrow*). **b** Axial CT image shows linear and extensive subcortical calcification in the bilateral parietal, occipital and frontal lobes (*arrow*). **c** Axial CT image shows marked brain sulcation and microlissencephaly (*arrow*). **d** Three-dimensional volume-rendered image viewed from the left lateral shows bone collapse, overriding sutures and occipital protuberance pointing upward (*arrow*)

being thick and chunky or fine and punctate, more commonly periventricular or subependymal in location (Fig. 19). Other locations include the basal ganglia, subcortical white matter and cerebellum [8, 60, 75]. Patients also present with anterior temporal lobe cysts, ventriculomegaly, white matter signal changes, polymicrogyria, lissencephaly, porencephaly and chorioretinitis (Fig. 20) [60].

Toxoplasmosis

Toxoplasmosis is the second most common TORCH-related infection following cytomegalovirus. Human infection is caused by the ingestion of undercooked infected meat, oral contact with infected feces, contaminated water/soil, or via the trans-placental route [76]. While the infection is mostly asymptomatic in immunocompetent people, it can be severe in the congenital form and in immunodeficient individuals. Neuroimaging of congenital toxoplasmosis is characterized by calcifications, ventriculomegaly, macro- or microcephaly, hydrocephalus, parenchymal destruction and microphthalmia (uni- or bilateral) (Fig. 21). Early gestational age infections result in more diffuse and large/coarse calcifications. Intracranial calcifications can occur anywhere (thalami and basal ganglia, periventricular, cerebral cortex), but tend to be more peripherally located as compared to those in cytomegalovirus infection [63, 76]. Resolution of intracranial calcifications has been described after antibiotic treatment [77]. White matter involvement is prevalent in the bilateral temporal, parietal and occipital regions with associated ex vacuo dilatation of the atrial portions of the lateral ventricles.

Zika virus

Zika virus is an emerging public health issue with several outbreaks reported in Africa, Southeast Asia, and more recently in the Americas, the Pacific and the Caribbean. Zika virus is transmitted by infected female mosquito vectors (i.e. *Aedes aegypti*). Other transmission modalities include maternal–fetal transmission, sexual intercourse, blood transfusion, laboratory exposure and organ transplantation [78].

Fig. 23 Axial nonenhanced CT image in a 9-year-old boy with frequent falls, motor developmental disorder, and perinatal human immunodeficiency virus (HIV) infection. Fine calcifications are located within the globus pallidus bilaterally (*arrow*)

Immunocompetent patients typically are not symptomatic but can experience a self-limiting illness characterized by a maculopapular rash, myalgia and small joint arthralgia, non-purulent conjunctivitis, and rarely Guillain–Barré syndrome [79]. Vertical maternal transmission is associated with several congenital birth defects such as collapsed appearance of the skull with overlapping sutures; cerebral volume loss; malformations of cortical development (i.e. cobblestone appearance, polymicrogyria, pachygyria); corpus callosum abnormalities (i.e. agenesis, dysgenesis); ventriculomegaly; cerebellar abnormalities in 6% (i.e. hemispheric hypoplasia or maldevelopment, vermian hypoplasia); brainstem hypoplasia/atrophy in 18%; delayed myelination; and parenchymal calcifications (Fig. 22) [80]. As opposed to other congenital infections, calcifications are mainly at the gray–white matter junction (up to 88% of cases) [81]. Other locations include the thalamus and basal ganglia (65%), periventricular regions (65%) and cortex (24%) [81].

Human immunodeficiency virus

The incidence of perinatal HIV infection has dramatically decreased worldwide in the last few years, though cases of vertical transmission are still diagnosed, especially in developing countries. HIV vertical transmission can occur transplacentally, during delivery or through breastfeeding. HIV-infected newborn babies are usually asymptomatic at birth, with the first neurologic manifestations typically presenting between 3 months and 10 years of age, such as developmental delay and failure to thrive [63]. Because HIV in children affects the immature brain, static or progressive encephalopathy can ensue; progressive leukoencephalopathy manifests with the classic triad of pyramidal tract motor deficits, acquired microcephaly, and delay/loss of developmental milestones [82]. Neuroimaging findings include cerebral atrophy, myelin loss (diffuse/multifocal) and mineralizing microangiopathy resulting in intracranial calcifications involving primarily the basal ganglia and subcortical white matter (frontal lobe predilection). Basal ganglia calcification, which was initially considered a marker of vertically transmitted infection, should instead be regarded as an acquired vascular injury. This calcification is usually bilaterally symmetrical in the basal ganglia (Fig. 23) but can also occur in the white matter and cerebellum. It is seen after 10 months of age and is often progressive. Children with high viral loads have the most pronounced calcification [83]. Later in the disease, children might develop vasculopathy with vascular ectasia and fusiform aneurysms [84]. As a consequence of acquired immunodeficiency syndrome (AIDS), progressive multifocal leukoencephalopathy, cytomegalovirus/varicella-zoster related encephalitis, central nervous system lymphoma, and secondary central nervous system tumors can ensue [63].

Conclusion

Intracranial calcification is common in childhood and may occur in the brain parenchyma, meninges, choroid plexus and within vessel walls. Physiological childhood intracranial calcification is characteristically not associated with any disease and is not an expected imaging finding in the neonatal period, but it increases in prevalence with incremental age. Chunky, extensive and multifocal intracranial calcifications are usually pathological in young children. Pathological intracranial calcification occurs in various pediatric neurologic conditions (static or progressive encephalopathies). These conditions can be further grouped into infectious, congenital, endocrine/metabolic, vascular, neoplastic and other miscellaneous causes. This review provides an approach for considering both the imaging findings and the available clinical information as they relate to the calcification and other associations for reaching a diagnosis.

Compliance with ethical standards

Conflicts of interest None

References

1. Institute of Medicine (US) Committee to Review Dietary Reference Intakes for Vitamin D and Calcium (2011) Dietary reference intakes for calcium and Vitamin D. The National Academies Press, Washington, DC
2. Marambaud P, Dreses-Werringloer U, Vingtdeux V (2009) Calcium signaling in neurodegeneration. Mol Neurodegener 4:20
3. Sama DM, Norris CM (2013) Calcium dysregulation and neuroinflammation: discrete and integrated mechanisms for age-related synaptic dysfunction. Ageing Res Rev 12:982–995
4. Zhivotovsky B, Orrenius S (2011) Calcium and cell death mechanisms: a perspective from the cell death community. Cell Calcium 50:211–221
5. Liu K, Ding L, Li Y et al (2014) Neuronal necrosis is regulated by a conserved chromatin-modifying cascade. Proc Natl Acad Sci U S A 111:13960–13965
6. McCartney E, Squier W (2014) Patterns and pathways of calcification in the developing brain. Dev Med Child Neurol 56:1009–1015
7. Kieffer SA, Gold LH (1974) Intracranial physiologic calcifications. Semin Roentgenol 9:151–162
8. Kıroğlu Y, Callı C, Karabulut N, Oncel C (2010) Intracranial calcifications on CT. Diagn Interv Radiol 16:263–269
9. Lago EG, Baldisserotto M, Hoefel Filho JR et al (2007) Agreement between ultrasonography and computed tomography in detecting intracranial calcifications in congenital toxoplasmosis. Clin Radiol 62:1004–1011
10. Livingston JH, Stivaros S, Warren D, Crow YJ (2014) Intracranial calcification in childhood: a review of aetiologies and recognizable phenotypes. Dev Med Child Neurol 56:612–626
11. Go JL, Zee CS (1998) Unique CT imaging advantages. Hemorrhage and calcification. Neuroimaging Clin N Am 8:541–558
12. Machida H, Tanaka I, Fukui R et al (2016) Dual-energy spectral CT: various clinical vascular applications. Radiographics 36:1215–1232
13. Nute JL, Le Roux L, Chandler AG et al (2015) Differentiation of low-attenuation intracranial hemorrhage and calcification using dual-energy computed tomography in a phantom system. Investig Radiol 50:9–16
14. Hu R, Daftari Besheli L, Young J et al (2016) Dual-energy head CT enables accurate distinction of intraparenchymal hemorrhage from calcification in emergency department patients. Radiology 280:177–183
15. American Society of Neuroradiology (2015) ACR–ASNR practice parameter for the performance of computed tomography (CT) of the brain revised 2015 (Resolution 20). https://www.asnr.org/guidelines-standards/acr-asnr-practice-parameter-for-the-performance-of-computed-tomography-ct-of-the-brain-revised-2015-resolution-20/. Accessed 27 Mar 2020
16. Greer M-LC (2018) Imaging of cancer predisposition syndromes. Pediatr Radiol 48:1364–1375
17. Sedghizadeh PP, Nguyen M, Enciso R (2012) Intracranial physiological calcifications evaluated with cone beam CT. Dentomaxillofac Radiol 41:675–678
18. Whitehead MT, Oh C, Raju A, Choudhri AF (2015) Physiologic pineal region, choroid plexus, and dural calcifications in the first decade of life. AJNR Am J Neuroradiol 36:575–580
19. Sapède D, Cau E (2013) The pineal gland from development to function. Curr Top Dev Biol 106:171–215
20. Kendall B, Cavanagh N (1986) Intracranial calcification in paediatric computed tomography. Neuroradiology 28:324–330
21. Adeeb N, Mortazavi MM, Tubbs RS, Cohen-Gadol AA (2012) The cranial dura mater: a review of its history, embryology, and anatomy. Childs Nerv Syst 28:827–837
22. McKinney AM (2017) Basal ganglia: physiologic calcifications. Atlas of normal imaging variations of the brain, skull, and craniocervical vasculature. Springer International Publishing, Cham, pp 427–440
23. Cox MA, Davis M, Voin V et al (2017) Pineal gland agenesis: review and case illustration. Cureus 9:e1314
24. Lun MP, Monuki ES, Lehtinen MK (2015) Development and functions of the choroid plexus-cerebrospinal fluid system. Nat Rev Neurosci 16:445–457
25. McKinney AM (2017) Dural calcifications: normal locations and appearances. Atlas of normal imaging variations of the brain, skull, and craniocervical vasculature. Springer International Publishing, Cham, pp 391–411
26. Qureshi PAAA, Qureshi MR, Rehan B (2017) Dehiscence of the lamina papyracea: MRI findings in correlation with CT appearance. Pak J Radiol 27:398–400
27. Pappamikail L, Rato R, Novais G, Bernardo E (2013) Chronic calcified subdural hematoma: case report and review of the literature. Surg Neurol Int 4:21
28. Daghighi MH, Rezaei V, Zarrintan S, Pourfathi H (2007) Intracranial physiological calcifications in adults on computed tomography in Tabriz, Iran. Folia Morphol (Warsz) 66:115–119
29. Murphy MJ (1979) Clinical correlations of CT scan-detected calcifications of the basal ganglia. Ann Neurol 6:507–511
30. Legido A, Zimmerman RA, Packer RJ et al (1988) Significance of basal ganglia calcification on computed tomography in children. Pediatr Neurosci 14:64–70
31. Herron J, Darrah R, Quaghebeur G (2000) Intra-cranial manifestations of the neurocutaneous syndromes. Clin Radiol 55:82–98
32. Randle SC (2017) Tuberous sclerosis complex: a review. Pediatr Ann 46:e166–e171
33. Northrup H, Krueger DA, International Tuberous Sclerosis Complex Consensus Group (2013) Tuberous sclerosis complex diagnostic criteria update: recommendations of the 2012 International Tuberous Sclerosis Complex Consensus Conference. Pediatr Neurol 49:243–254
34. von Ranke FM, Faria IM, Zanetti G et al (2017) Imaging of tuberous sclerosis complex: a pictorial review. Radiol Bras 50:48–54
35. Davis PE, Filip-Dhima R, Sideridis G et al (2017) Presentation and diagnosis of tuberous sclerosis complex in infants. Pediatrics 140:e20164040
36. Umeoka S, Koyama T, Miki Y et al (2008) Pictorial review of tuberous sclerosis in various organs. Radiographics 28:e32
37. Gallagher A, Madan N, Stemmer-Rachamimov A, Thiele EA (2010) Progressive calcified tuber in a young male with tuberous sclerosis complex. Dev Med Child Neurol 52:1062–1065
38. Martin N, de Broucker T, Cambier J et al (1987) MRI evaluation of tuberous sclerosis. Neuroradiology 29:437–443
39. Menor F, Martí-Bonmatí L, Mulas F et al (1992) Neuroimaging in tuberous sclerosis: a clinicoradiological evaluation in pediatric patients. Pediatr Radiol 22:485–489
40. Baron Y, Barkovich AJ (1999) MR imaging of tuberous sclerosis in neonates and young infants. AJNR Am J Neuroradiol 20:907–916
41. Koh S, Jayakar P, Dunoyer C et al (2000) Epilepsy surgery in children with tuberous sclerosis complex: presurgical evaluation and outcome. Epilepsia 41:1206–1213
42. Inoue Y, Nemoto Y, Murata R et al (1998) CT and MR imaging of cerebral tuberous sclerosis. Brain Dev 20:209–221
43. Crino PB, Nathanson KL, Henske EP (2006) The tuberous sclerosis complex. N Engl J Med 355:1345–1356
44. Hodgson N, Kinori M, Goldbaum MH, Robbins SL (2017) Ophthalmic manifestations of tuberous sclerosis: a review. Clin Exp Ophthalmol 45:81–86
45. Higueros E, Roe E, Granell E, Baselga E (2017) Sturge-Weber syndrome: a review. Actas Dermosifiliogr 108:407–417
46. Singh AK, Keenaghan M (2020) Sturge-Weber syndrome. StatPearls Publishing, Treasure Island

47. Comi AM (2007) Sturge-Weber syndrome and epilepsy: an argument for aggressive seizure management in these patients. Expert Rev Neurother 7:951–956
48. Akpinar E (2004) The tram-track sign: cortical calcifications. Radiology 231:515–516
49. Roy U, Panwar A, Mukherjee A, Biswas D (2016) Adult presentation of Dyke-Davidoff-Masson syndrome: a case report. Case Rep Neurol 8:20–26
50. Frantzen C, Klasson TD, Links TP, Giles RH (1993) Von Hippel-Lindau syndrome. In: Pagon RA, Adam MP, Ardinger HH et al (eds) GeneReviews. University of Washington, Seattle. http://www.ncbi.nlm.nih.gov/books/NBK1463/. Accessed 27 Mar 2020
51. Maher ER (1994) Von Hippel-Lindau disease. Eur J Cancer 30A: 1987–1990
52. Chittiboina P, Lonser RR (2015) Von Hippel-Lindau disease. Handb Clin Neurol 132:139–156
53. Lonser RR, Glenn GM, Walther M et al (2003) von Hippel-Lindau disease. Lancet 361:2059–2067
54. Diaz RC, Amjad EH, Sargent EW et al (2007) Tumors and pseudotumors of the endolymphatic sac. Skull Base 17:379–393
55. Thalakoti S, Geller T (2015) Basal cell nevus syndrome or Gorlin syndrome. Handb Clin Neurol 132:119–128
56. Pino LC, Balassiano LK, Sessim M et al (2016) Basal cell nevus syndrome: clinical and molecular review and case report. Int J Dermatol 55:367–375
57. Kazemi M, Salehi M, Kheirollahi M (2016) Down syndrome: current status, challenges and future perspectives. Int J Mol Cell Med 5:125–133
58. Annus T, Wilson LR, Acosta-Cabronero J et al (2017) The down syndrome brain in the presence and absence of fibrillar β-amyloidosis. Neurobiol Aging 53:11–19
59. Ieshima A, Kisa T, Yoshino K et al (1984) A morphometric CT study of Down's syndrome showing small posterior fossa and calcification of basal ganglia. Neuroradiology 26:493–498
60. Fink KR, Thapa MM, Ishak GE, Pruthi S (2010) Neuroimaging of pediatric central nervous system cytomegalovirus infection. Radiographics 30:1779–1796
61. Klase ZA, Khakhina S, Schneider ADB et al (2016) Zika fetal neuropathogenesis: etiology of a viral syndrome. PLoS Negl Trop Dis 10:e0004877
62. Maldonado YA, Read JS, Committee on Infectious Diseases (2017) Diagnosis, treatment, and prevention of congenital toxoplasmosis in the United States. Pediatrics 139:e20163860
63. Neuberger I, Garcia J, Meyers ML et al (2018) Imaging of congenital central nervous system infections. Pediatr Radiol 48:513–523
64. Numazaki K, Fujikawa T (2003) Intracranial calcification with congenital rubella syndrome in a mother with serologic immunity. J Child Neurol 18:296–297
65. Chantler JK, Davies MA (1987) The effect of antibody on rubella virus infection in human lymphoid cells. J Gen Virol 68:1277–1288
66. Tien RD, Felsberg GJ, Osumi AK (1993) Herpesvirus infections of the CNS: MR findings. AJR Am J Roentgenol 161:167–176
67. Noorbehesht B, Enzmann DR, Sullender W et al (1987) Neonatal herpes simplex encephalitis: correlation of clinical and CT findings. Radiology 162:813–819
68. Petribu NCL, Fernandes ACV, Abath MB et al (2018) Common findings on head computed tomography in neonates with confirmed congenital Zika syndrome. Radiol Bras 51:366–371
69. Moore CA, Staples JE, Dobyns WB et al (2017) Characterizing the pattern of anomalies in congenital Zika syndrome for pediatric clinicians. JAMA Pediatr 171:288–295
70. Anderson JL, Levy PT, Leonard KB et al (2014) Congenital lymphocytic choriomeningitis virus: when to consider the diagnosis. J Child Neurol 29:837–842
71. Deasy NP, Jarosz JM, Cox TC, Hughes E (1999) Congenital varicella syndrome: cranial MRI in a long-term survivor. Neuroradiology 41:205–207
72. Takayama M (1994) Reactivity of varicella-zoster virus subunit antigens in enzyme-linked immunosorbent assay to sera from varicella, zoster, and herpes simplex virus infections. Med Microbiol Immunol 183:1–11
73. Cheeran MC-J, Lokensgard JR, Schleiss MR (2009) Neuropathogenesis of congenital cytomegalovirus infection: disease mechanisms and prospects for intervention. Clin Microbiol Rev 22:99–126
74. van der Knaap MS, Vermeulen G, Barkhof F et al (2004) Pattern of white matter abnormalities at MR imaging: use of polymerase chain reaction testing of Guthrie cards to link pattern with congenital cytomegalovirus infection. Radiology 230:529–536
75. Barkovich AJ, Lindan CE (1994) Congenital cytomegalovirus infection of the brain: imaging analysis and embryologic considerations. AJNR Am J Neuroradiol 15:703–715
76. Khan K, Khan W (2018) Congenital toxoplasmosis: an overview of the neurological and ocular manifestations. Parasitol Int 67:715–721
77. Patel DV, Holfels EM, Vogel NP et al (1996) Resolution of intracranial calcifications in infants with treated congenital toxoplasmosis. Radiology 199:433–440
78. Karkhah A, Nouri HR, Javanian M et al (2018) Zika virus: epidemiology, clinical aspects, diagnosis, and control of infection. Eur J Clin Microbiol Infect Dis 37:2035–2043
79. Faria NR, Azevedo RDSDS, Kraemer MUG et al (2016) Zika virus in the Americas: early epidemiological and genetic findings. Science 352:345–349
80. de Fatima Vasco Aragao M, van der Linden V, Brainer-Lima AM et al (2016) Clinical features and neuroimaging (CT and MRI) findings in presumed Zika virus related congenital infection and microcephaly: retrospective case series study. BMJ 353:i1901
81. Soares de Oliveira-Szejnfeld P, Levine D, Melo AS et al (2016) Congenital brain abnormalities and Zika virus: what the radiologist can expect to see prenatally and postnatally. Radiology 281:203–218
82. Van Rie A, Harrington PR, Dow A, Robertson K (2007) Neurologic and neurodevelopmental manifestations of pediatric HIV/AIDS: a global perspective. Eur J Paediatr Neurol 11:1–9
83. George R, Andronikou S, du Plessis J et al (2009) Central nervous system manifestations of HIV infection in children. Pediatr Radiol 39:575–585
84. Cantey JB, Sisman J (2015) The etiology of lenticulostriate vasculopathy and the role of congenital infections. Early Hum Dev 91: 427–430